5-2007

Energy Absorption of Sine Wave Beams Subjected to Axial Impact Loading

Robert Smith
Clemson University, hsrober@clemson.edu

ENERGY ABSORPTION OF SINE WAVE BEAMS SUBJECTED TO AXIAL IMPACT LOADING

A Thesis
Presented to
the Graduate School of
Clemson University

In Partial Fulfillment
of the Requirements for the Degree
Master of Science
Mechanical Engineering

---

by
Robert Harvin Smith Jr.
May 2007

Accepted by:
Dr. Sherrill Biggers, Committee Chair
Dr. Lonny Thompson
Dr. Gang Li

ABSTRACT

Structural impact is an area of research that has become very important in today's society, specifically in transportation systems. Use of energy absorbers as devices to absorb impact energy has been, and continues to be the focus of extensive research. The goal of energy absorber design is to create an absorber that will remove kinetic energy from the system in an efficient and reliable way while not imposing high force magnitudes on the moving body. Until now, the structural response of energy absorbers under an impact loading has concentrated on thin-walled prismatic structures, such as square and cylindrical tubes, as well as thin-walled tapered tubes. The sine wave beam has been previously investigated as an energy absorber under lateral impacting situations, however had yet to be studied under the axial impact loading condition. The aim of this thesis was to investigate the structural response and resulting energy absorbing performance of the sine wave beam subjected to axial impact and to compare this performance to that of previously considered thin-walled prismatic designs. Detailed finite element models were created and subsequently validated using existing theoretical and numerical models. These FE models were used to simulate the response of the sign wave beam and prismatic structures undergoing an axial impact. A parametric analysis was performed using the thickness of the upper and lower flange plates and the web, the amplitude of the sine wave web, and the number of sine wave periods along the length of the beam. The results show that the energy absorbing performance of the sine wave beam is affected greatly by the thickness of the structural components. Additionally, the web amplitude and period number play a vital role in the structural response and resulting

energy absorption exhibited by the structure. Comparing the sine wave beam to typical prismatic tubes, advantages can be observed. The force felt by the impacting body is less for all of the sine wave beams than for any of the prismatic structures, when absorbing the same amount of kinetic energy. The sine wave beam also has greater stroke efficiency than the typical prismatic structures. The results indicate that larger number of design parameters in the sine wave beam therefore allows effective control over the crush deformation and resulting energy absorption compared to the prismatic absorber designs.

DEDICATION

This thesis is dedicated to my mother for all of her help and support throughout my college career. Without her, I would not be where I am today.

ACKNOWLEDGEMENTS

I would like to thank Dr. Sherrill Biggers for his guidance and assistance throughout this project. His support is greatly appreciated and has been an invaluable contribution to this work.

TABLE OF CONTENTS

Table of Contents (Continued)

Table of Contents (Continued)

LIST OF FIGURES

List of Figures (Continued)

List of Figures (Continued)

List of Figures (Continued)

NOMENCLATURE

a_0	-	Acceleration of the center of gravity of free-free beam
A_0	-	Original cross sectional area of absorber
C	-	Side width
D	-	Characteristic strain-rate used in Cowper-Symonds relation, material constant
d	-	Crush distance
d_{max}	-	Maximum crush distance
$\dot{\varepsilon}$	-	Strain-rate
E	-	Young's modulus
E_{abs}	-	Total kinetic energy absorbed
E_{cl}	-	Energy absorber per unit crush length
E_m	-	Kinetic energy absorbed per unit mass
F	-	Force
$F(t)$	-	Impulsive force
F_d	-	Dynamic collapse force
F_{dmc}	-	Dynamic mean crushing force
F_E	-	Crush force efficiency
F_{mean}	-	Mean crushing force
F_{peak}	-	Peak force
H, h	-	Wall thickness
L	-	Length

Nomenclature (Continued)

l	-	Original, undeformed length of energy absorber
m	-	Mass of energy absorber
M_0	-	Fully plastic bending moment
P_b	-	Buckling force applied for initial imperfection analysis
P_m	-	Theoretical mean force
q	-	Strain-rate sensitivity of a material
S_E	-	Stroke efficiency
S_{lm}	-	Stroke length per unit mass
t	-	Time
ε_p	-	Plastic strain
v	-	Poisson's ratio
ρ	-	Mass per unit length, density
σ_0	-	Average of material's yield and ultimate stresses
σ_{cr}	-	Mean crushing stress
σ_d	-	Dynamic yield stress
σ_s	-	Static yield stress
σ_t	-	True stress
σ_y	-	Yield stress

1. INTRODUCTION

Structural impact is an area of research that has become very important in today's society, specifically in transportation systems. This loading condition can be explored using various techniques including theoretical, experimental, and computational methods like the finite element method. When a structure undergoes deformation, it absorbs a given amount of energy based on its deformation mode. Structures that are designed to absorb energy under given conditions are called energy absorbers. The goal of energy absorber design is to create an absorber that will remove kinetic energy from the system in an efficient and reliable way while not imposing high force magnitudes on the moving body. The deformation mode of the absorber should be predictable and repeatable for maximum efficiency in design. This mode can be examined through study of geometric performance and optimization. A validated finite element analysis (FEA) model was used for this investigation. This project sets out to explore the area of geometrically designed impact energy absorbing structures.

1.1 Fundamentals of Impact Mechanics and Structural Crashworthiness

In order to understand the design of an energy absorbing structure it is necessary to understand the more general topics of impact mechanics and structural crashworthiness. An impact load differs from that of quasi-static (gradually applied) load in three major areas: stress wave propagation, inertial effects, and strain-rate. These three factors become significant as the type of load changes from quasi-static to impulsive (Lu & Yu 2003). As the subjects of impact mechanics and structural crashworthiness are

vital to the analysis of an energy absorbing structure, these two topics are detailed further in Sections 1.1.1 and 1.1.2.

1.1.1 Impact Mechanics

For the purpose of this research, the effects of dynamic loading must be understood. As previously stated, dynamic loads are very different from quasi-static loads. When a dynamic load is applied to an object, it results in a suddenly gained particle velocity inside the material called a stress wave. While there are two kinds of stress waves, elastic and plastic, only plastic waves affect a structure's deformation. An elastic stress wave occurs when the resulting stress from the impact, remains below the yield stress of the material. If that stress goes above the yield stress however, a plastic stress wave will appear. Propagation of plastic stress waves can affect energy absorption of a structure in various ways inducing failure. Three of the most common types of wave propagation and their resulting failures are described here. If in the region where impact occurs the stress experienced causes local plastic collapse, then the compressive plastic stress wave is to blame. The remainder of the structure may only experience elastic stress waves and will remain undamaged. When a structure experiences a compressive elastic wave reaching a free edge, the wave will be reflected back as a tensile wave. In the case of a low tensile strength, brittle material, this tensile wave may cause a fracture in the structure away from the free edge. This type of failure is called spalling and will dissipate kinetic energy by fractured material breaking away from the structure. Lastly, if a compressive elastic stress wave reaches a fixed edge, the wave will be reflected back as a compressive wave with stress doubled in magnitude. This phenomenon may cause the initial deformation of certain structures to be initiated closer to these fixed ends than the

area where impact occurred (Lu & Yu 2003). For additional information regarding plastic wave propagation the reader can consult Johnson and Yu (1989).

Inertial effects have great influence on the deformation mode of a structure causing different responses of material under dynamic versus quasi-static loading. Under a quasi-static load, an ideal rigid-plastic structure can sustain loading up to its yielding force. When this load limit is reached, the structure will plastically deform and the load redistributed until it ultimately fails. Under dynamic loading conditions, for example impulsive loading, the force is only applied for a finite amount of time and changes in magnitude depending on the structural response. This may lead to an ultimate failure of the structure, but not always. The energy dissipated by the structure is inversely proportional to its mass and unique deformation occurs. For the derivation of the energy dissipation of a system subjected to an impulsive loading, the reader is referred to Lu & Yu (2003). The effect inertia can best be illustrated by an example of a free-free beam of length *2L* having force applied to the center. Since the beam is not supported, it cannot experience any quasi-static force greater than zero. But if the application of a dynamic force *F(t)* is a step force of magnitude *F*, the beam will move in the direction of the force. The acceleration of the center of gravity of the beam is given by the equation, $a_o = F / 2\rho L$, where ρ is the mass per unit length of the beam. The application of the force in the center of the beam creates a bending moment, and if the magnitude of *F* reaches the dynamic collapse force F_d, a plastic hinge will form. There is no static collapse force in the case of the free-free beam, and only dynamic loading will cause this possible collapse. The loading condition results in a mechanism of two smaller beams with length *L,* rotating about the plastic hinge with angular acceleration, α, for each half

of the beam. This result is unattainable through a quasi-static load and the accelerations experienced in the material lead to an increase in strain rate.

Strain-rate and the effect of strain-rate on structures and materials is the third major factor that distinguishes dynamic from quasi-static loading. When a structure is loaded dynamically, it will deform rapidly resulting in large strain-rates. This phenomenon is important as many engineering materials' mechanical properties have strain-rate dependence. Therefore, the loading capacity of a structure experiencing dynamic forces will depend on the speed of loading and the dynamic response. To account for this phenomenon many constitutive equations have been derived. However the most common, and the one used in the majority of today's FEA packages, is the Cowper-Symonds equation. This relation, given in Equation (1.2.1), takes into account two separate material constants.

$$\frac{\sigma_d}{\sigma_s} = 1 + \left(\frac{\dot{\varepsilon}}{D} \right)^{1/q} \tag{1.2.1}$$

The first constant, D, is the characteristic strain-rate at which the dynamic yield stress of the material is equal to twice the static yield stress. The second constant, q, is a measure of the rate sensitivity of the material in question. Generalized tables of these two constants have been created for numerous engineering materials having strains less than or equal to 5% (Lu & Yu 2003). Unfortunately, most impact applications involve strains much larger than 5% and therefore a slight change to this previous relation has to be made. Instead of using just the static yield stress in this relation, incorporating the static ultimate stress produces results that are more accurate. The corresponding values for D and q must also be altered slightly when using this modified equation (Nagel 2005; Abramowicz & Jones 1984; 86; Reid & Reddy 1986; Reid et al. 1986).

For more information regarding these relations and the effect of strain-rate on material deformation the reader is referred to Lu & Yu (2003) and Jones (2001; 1999; 89).

1.1.2 Structural Crashworthiness

Structural crashworthiness is a term that refers to the performance of a structure under an impact loading. Lu and Yu (2003) define this specifically as:

"..the quality of response of a vehicle when it is involved in or undergoes an impact. The less damaged the vehicle and/or its occupants and contents after the given event, the higher the crashworthiness of the vehicle or the better its crashworthy performance."

High crashworthiness is the ultimate goal of all impact research. It is necessary to understand the impact deformation of a structure under various conditions first, before learning how to improve its crashworthiness. Structures must be designed with a prescribed level of crashworthiness in order to be considered safe. One of the requirements of a crashworthy structure is its ability to dissipate kinetic energy without compromising the integrity of the structure or its occupants (Farley 1992). Kinetic energy dissipation is the focal point of this research and energy absorbers can be investigated using the characteristics described in the following section.

1.2 Energy Absorber Characteristics

Desired energy absorber characteristics vary depending on the implementation criteria and the type of impact that will be experienced. Each application calls for certain energy absorbing properties and the type of absorber should be selected based on its performance. The eight major energy absorbing characteristics described here are:

- Energy absorbed per unit mass

- Dynamic crushing force
- Dynamic mean crushing force
- Energy absorbed per unit crush length
- Crush force efficiency
- Stroke efficiency
- Stroke length per unit mass
- Mean crushing stress

Each of the characteristics in absorber performance carries a different weight based on the application (Nagel 2005). These are further detailed in the following sections and some are later used to quantify the performance of energy absorber designs in this thesis.

1.2.1 Energy absorbed per unit mass

The energy absorbed per unit mass, denoted by E_m (kJ/kg), is also referred to as the specific energy. This value is obtained by the following equation:

$$E_m = E_{abs} / m \tag{1.2.2}$$

where E_{abs} (kJ) is the total energy absorbed, and m (kg) is the mass of the undeformed energy absorber. This value is completely dependent on the mode of deformation of the energy absorber. If a structure deforms through axial crushing, it will experience more plastic deformation than if it were to undergo lateral crushing or Euler-type, global buckling. This relationship can be particularly important in cases where weight is critical, such as aerospace or lightweight engineering applications. It should be noted that just because a structure has a high specific energy, this fact alone does not necessarily mean it is best suited for all applications. A structure made of mild steel may weigh more than a structure made of a composite material; but one must look at the total

energy absorbed for each absorber. In order for the total energy to be equal, the composite structure may need to be quite a bit bigger than the mild steel structure, therefore requiring more space for implementation, which may not be available.

1.2.2 Dynamic mean crushing force

The dynamic mean crushing force is calculated by dividing the total energy absorbed E_{abs} (J), by the crush distance, d (m). The crush distance is defined as the magnitude of the shortening of the absorber at the instant the energy absorbed is being measured. The maximum crush distance achievable for a given crushing case is where compaction begins to occur and is called d_{max} (m). Compaction is the phenomenon caused by the material being crushed, piling up near the end of the absorber's stroke. When this occurs the force experienced on the impacting body increases greatly leading to greater decelerations experienced by the passengers. Ideally the absorber is designed to absorb enough energy prior to compaction so the increased deceleration is not an issue. In this thesis, the dynamic mean crushing force is used for comparison between the different absorber designs

1.2.3 Dynamic crushing force

The dynamic crushing force is the actual force the energy absorber applies to the impacted surface during the crushing process. The lower this value is, the less detrimental the crush process will be on the involved parties. This characteristic is different from the dynamic mean crushing force in that it is an actual time dependent force, instead of a calculated average force. .

1.2.4 Energy absorbed per unit crush length

The energy absorbed per unit crush length, E_{cl} (kJ/m), can be a very important factor when the length of the energy absorber must be limited. There are a few different ways to calculate this parameter, including dividing the energy absorbed by the undeformed length of the energy absorber, or dividing the energy absorbed by the maximum crush distance experienced in the deformation. In this thesis this parameter is calculated using the latter method in order to provide a head to head comparison of all the energy absorbers studied.

1.2.5 Crush force efficiency

The crush force efficiency is calculated by simply dividing the mean crushing force by the peak force experienced during deformation, or:

$$F_E = F_{mean} / F_{peak} \tag{1.2.3}$$

This relation is important to consider when occupant protection is a priority, since the occupants experience all forces present during the impact. Maximizing this relation will lead to greater occupant protection with the least amount of peak force being transmitted to the passenger compartment. Ways of reducing the peak force include introducing triggering mechanisms such as initial indentations or tapers into the original geometry to aid in controlling the deformation of the energy absorber.

1.2.6 Stroke efficiency

Stroke efficiency, S_E, is a way of measuring how the absorber performs axially in terms of the crush length and total length. This relationship is expressed by the following ratio:

$$S_E = d_{\max} / l \tag{1.2.4}$$

where d_{max} (mm) is the maximum crush distance, and l (mm) is the original, undeformed length of the absorber. Generally speaking, axially crushed, thin walled members have lower stroke efficiency than cellular structures due to compaction. Cellular materials, such as foam, have more empty space than thin walled members, which allows for greater compressibility. Optimally the absorber will deform over its entire length, maximizing this parameter. A longer crush distance utilized by an absorber equates to a lower crushing force required to absorb the same amount of energy.

1.2.7 Stroke length per unit mass

The stroke length per unit mass, S_{lm} (mm/kg), relates to the energy absorbed per unit mass by allowing comparison of absorbers made from different materials with different densities. This relation is given in Equation (1.2.5):

$$S_{lm} = d_{\max} / m \tag{1.2.5}$$

1.2.8 Mean crushing stress

The mean crushing stress is calculated by the following equation:

$$\sigma_{cr} = F_{mean} / A_0 \tag{1.2.6}$$

where, σ_{cr} (MPa) is the mean crushing stress, F_{mean} (kN) is the mean crushing force, and A_0 (mm^2) is the original cross sectional area of the absorber. While this may be an important characteristic of energy absorbers, it is only applicable to prismatic absorbers which have a uniform cross sectional area down their entire length (Nagel 2005). This is not the case with the energy absorbers being described in this thesis and therefore will not be used as a performance measure.

There are a few final characteristics that all energy absorbers should possess, but are not quantifiable by an equation or relation. The first of these is that all energy

absorbing structures should have stable and repeatable deformation modes. This is because the exact loading conditions are quite often unknown so therefore the energy absorber should be tailored to fit a wide variety of loading conditions while still absorbing the maximum amount of energy. The deformation should be repeatable so that it can be predictable in its application. Also energy absorbers should be easy to manufacture, implement and maintain to be cost-effective. This is especially true for energy absorbers that are permanently deformed after impact, and have to be replaced (Lu & Yu 2003).

1.3 Description of Previous Work

The following section provides a review of the current literature on energy absorbing structures and their analysis. The absorbers have been divided into five major categories, listed below, and will be described separately in the following sections.

- Thin-walled prismatic structures
- Tapered tubes
- Cellular structures
- Foam and foam-filled structures

There is also much literature relating to energy absorption of other structures and materials. However, in order to narrow the scope of this study, these have not been presented here. In addition to the discussion of the absorbers themselves, the various analysis techniques for calculating energy absorber performance are presented here. Theoretical, experimental, and computational methods are the accepted analysis techniques used to compare the performance of energy absorbers. In recent times, the focus of the research into energy absorbers has shifted to the use of FEA to perform

investigations into proposed structures and their effectiveness. The FEA simulations must be validated using experimental and/or theoretical techniques, and are well suited for parametric studies of complex geometries or loading conditions. For more information on energy absorption the reader is referred to the book by Lu and Yu (2003). For a more current review of thin-walled energy absorbing structures the reader is also referred to Abramowicz (2003).

1.3.1 Thin-walled prismatic structures

This category includes all straight, thin-walled, tubular structures with cross sections including square, rectangular, circular, triangular, hexagonal, and octagonal. The loading conditions discussed here are split into two types, axial crushing and oblique loading. Axially crushed thin-walled tubes have been studied extensively for quite some time and still today are considered the most common type of energy absorber (Alghamdi 2001). These tubes have been used frequently in various applications such as behind car bumpers and at the base of elevator shafts. The materials used in thin-walled tubes can vary, however the most common are steel, aluminum alloy, and Fiber Reinforced Composites (FRCs). Tubes made of isotropic materials such as steel and aluminum alloy have been studied for many years now, whereas composite materials are a relatively new area of study. Metallic structures absorb energy through their ductility, by plastically deforming while composite structures dissipate energy through brittle fracture of the fibers contained in the material and delamination.

Metallic tubes can deform in many different ways in order to absorb energy. The most prevalent deformations methods are axial crushing, axial inversion, axial splitting,

lateral bending, lateral indentation, and lateral flattening. The axial deformations are the most efficient modes for energy absorption and therefore will be the focus of this review.

Axial crushing is probably the most common deformation method used with thin-walled tubes because of its high energy absorbing capacity and relatively constant crushing force. The major focus of study has been with square and circular cross section tubes. Circular cross section tubes deform in different modes depending on their geometric features. These modes of deformation are referred to as axisymmetric (concertina) crushing, non-axisymmetric (diamond), and global buckling. Axisymmetric crushing is the most efficient mode of deformation but results in a higher dynamic crushing force. Non-axisymmetric crushing absorbs less energy per unit length, and has a lower crushing force as a result. Global buckling is very inefficient in energy absorption and should be avoided at all costs. The mode of deformation depends on the ratios of diameter to wall thickness, and length to wall thickness. Tube material and boundary conditions on the tube affect its performance as well, but less severely than the geometric ratios. For more information regarding the axial crushing of circular cross section tubes, the reader is referred to Abramowicz & Jones (1984) and Lu & Yu (2003).

The axial crushing of square and rectangular tubes is classified into two deformation modes: symmetric and non-symmetric. The ratio of side width, C, to wall thickness, H, determines this mode. Jones (1989) showed that for values of C/H greater than 40.8, symmetric crushing occurs, where values lower than 7.5 cause extensional buckling (non-symmetric) to occur. For values between 7.5 and 40.8, there exists a mixed mode of deformation called B-type progressive buckling. Within either mode of deformation, two types of collapse elements exist: Type I and Type II. These two types

of collapse elements exhibit different energy absorption properties. Type I undergoes considerably less plastic deformation than Type II. With lower plastic deformation, less crush force is experienced, and therefore less negative effects are felt by the impacting body. The symmetric crushing mode consists of four Type I crushing elements, where the extensional crushing mode consists of four Type II crushing elements. The mixed, B-type crushing mode contains seven Type I and one Type II collapse elements. For more information regarding the axial crushing of square and rectangular tubes, the reader is referred to Jones (1989), Lu & Yu (2003), and Reid & Reddy (1986).

Numerous engineers have also investigated axial crushing of other various prismatic geometries. These additional cross sectional geometries consist of hexagonal, octagonal, triangular, multicell rectangular, and other complex shapes. Sun et al. (2004) investigated the performance of triangular and hexagonal cross sectional shapes of equal cross sectional volume compared to circular and square ones. Their findings stated that the triangular tube absorbed the same amount of kinetic energy with lower dynamic mean force than the other geometries. The square tube had higher dynamic mean force but remained lower than the hexagonal tube. The highest dynamic mean force exhibited was that of the circular tube. The equilateral triangle was found to be the optimal triangular cross section (Sun et al. 2004).

Axially inverting a tube is a less common method for plastically deforming a thin-walled tube. This process is performed by placing a die on the end of a tube and forcing the tube over the die. The tube will plastically stretch and curl either inward or outward, depending on the shape of the die. This method has been shown to exhibit beneficial energy absorbing qualities however will not be further discussed here. Axial splitting is

another method of energy absorption very similar to axial inversion. The difference between axial inversion and axial splitting is that the die used to curl the tube has larger radius causing ductile tearing of the tube instead of just plastic deformation. For additional information on axial inversion and axial splitting the reader is referred to the book by Lu & Yu (2003).

Composite materials deform with a completely different deformation mechanism due to the composition of the material. Composites are made up of layers of fibrous materials, such as carbon fiber or Kevlar, that have been attached together using a laminate of some sort. The major advantage of composite materials over metallic materials is the reduction in weight. Compared to steel or aluminum, the energy absorbed per unit weight can be as much as 500% (Pinho et al. 2004). Stand alone composite structures as well as composite wrapped metallic tubes have been studied in depth, and have presented some interesting and beneficial results. Song et al. (2000) studied the impact energy absorption of glass/epoxy composite externally wrapped circular metal tubes. They found four collapse modes are present with influencing factors being strain rate, composite wall thickness, fiber ply orientation, as well as the mechanical properties of the metal. They concluded their work by modifying an existing theoretical model to include the dynamic effect of impact loadings. Schultz (1998) performed a full investigation into the energy absorption capacity of graphite-epoxy composite tubes. He concluded that the energy absorbed by a composite tube was based on many factors: crush rate, cross sectional geometry, fiber stacking sequences, and fiber materials. For additional information on composite tube crush deformation and energy absorption, the reader is referred to Farley (1989), and Schultz (1998).

1.3.2 Tapered tubes

Literature regarding tapered tubes of various cross sections, angles, and numbers of tapers focuses mainly on two- and four-tapered (frusta) tubes. Most recently, Nagel (2005) performed an in depth investigation into tubes having one, two, three, and four tapers of varying taper angles. The behavior of tapered tubes under axial loading is advantageous to that of straight (non-tapered) tubes for a few reasons. The first advantage is a tapered tube gives two additional geometric parameters. These parameters can be controlled to vary the response of the tube and they are: taper angle and number of tapers. The second advantage is tapered tubes are less affected by lateral inertia effects than straight tubes. A tube with a triple taper has been found to absorb the most energy for a given crush distance. Rectangular tapered tubes as a whole have higher dynamic crush force efficiency than rectangular straight tubes. Under oblique loading when the angle of applied load is increased, the energy absorbed by straight and tapered tubes decreases significantly. However, the addition of a taper to the tube will produce more positive results under the oblique loading. The mean load-deflection response remains more constant with the tapered tube than with the straight one. Therefore, the tapered tube is said to be more crashworthy in vehicular applications where oblique loadings are experienced (Nagel 2005; Reid and Reddy 1986; and, Mamalis et al. (1989; 2001).

1.3.3 Honeycombs

Honeycomb structures fall under the category of cellular structures and are frequently used in a wide variety of energy absorbing applications. The typical honeycomb shape has a hexagonal cell, but other cell shapes do exist. All honeycomb structures consist of two dimensional cells making their energy absorbing characteristics

change if loading is in-plane, out-of-plane, or a mixture of the two. Honeycombs can be made of many different materials including thermoplastics, injection molded polyolefin, elastomeric material, sheet steel or aluminum; the most common of these are sheet steel and aluminum (Nagel 2005). When characterizing cellular materials, one of the most important parameters is the relative density. This value is obtained by dividing the overall density of the cellular material by the density of the solid of which the material consists. Two additional relevant properties to consider when characterizing the energy absorption of honeycomb structures are called the plateau stress and the densification strain. For more information regarding the general qualification and energy absorbing performance of honeycomb structures the reader is referred to the books by Lu & Yu (2003) and Gibson & Ashby (1997).

1.3.4 Foam and foam-filled structures

Foam is another cellular material that has been studied for its energy absorbing properties. Foam can be made of different materials and the most common found in energy absorbers are metal and polymer. As a cellular structure, foam has a three dimensional cell instead of a honeycomb's two dimensional cell. This allows foam to have advantageous energy absorbing properties in all three planes of space. When looking at the energy absorbing properties of foam and foam filled structures two parameters are the most important: relative density and cell-wall material. These two factors affect the performance of the foam greatly and their relationship to each other will depend on the loading application.

Introducing foam to the interior of a thin-walled tube will increase the overall energy absorption capacity of the tube. The buckling wave present in the tube will be

reduced, and the corresponding mean crushing force will be slightly increased. The bending stiffness of the deformed cross section is also increased, which will decrease the likelihood of global buckling (Abramowicz & Wierzbicki 1988). Børvik et al. (2003) tested aluminum foam-filled aluminum tubes under axial and oblique loads. They found that the addition of the foam increased the specific energy from an empty tube under axial crushing, but decreased it under oblique loading. They also noted that the load angle played a significant role in the energy absorption, with an increase in angle leading to a decrease in energy absorption (Børvik et al. 2003). For additional information regarding the energy absorbing performance of foam filled structures, the reader is referred to Reddy & Wall (1988), Heyerman (2000), Børvik et al. (2003), and Reyes et al. (2004).

1.4 Need for Further Work

This literature review has introduced all of the topics that are relevant to the study of energy absorbing structures. The topics of impact mechanics and structural crashworthiness were covered, with the focus being on axial deformation of thin-walled tubes. The information available in open literature focuses on prismatic, closed section structures with no mention of open section absorbers. This raises the question: How will an open section absorber perform under an impact load?

In addition to the absorbers, the solving techniques used for the structural response under dynamic loading have been explored. Three methods are available for calculating the energy absorption of a structure: theoretical, experimental, and computational. The most recent, and the one used in this thesis, is the computational method called the finite element method. This method is capable of performing detailed

parametric analyses with very little change in model accuracy or cost of prototype building. The aim of this thesis is to computationally explore the response of an open section absorber subjected to an impact load situation.

2. MODEL DESCRIPTION

2.1 Structural and Material Model Descriptions

To understand the investigation presented here, an in-depth understanding of the physical model is required. This structure is an open section beam that has a sinusoidally shaped web fixed between the upper and lower plates. A representation of this sine wave beam, hereafter referred to as SWB, is given in Figure 2.1.1.

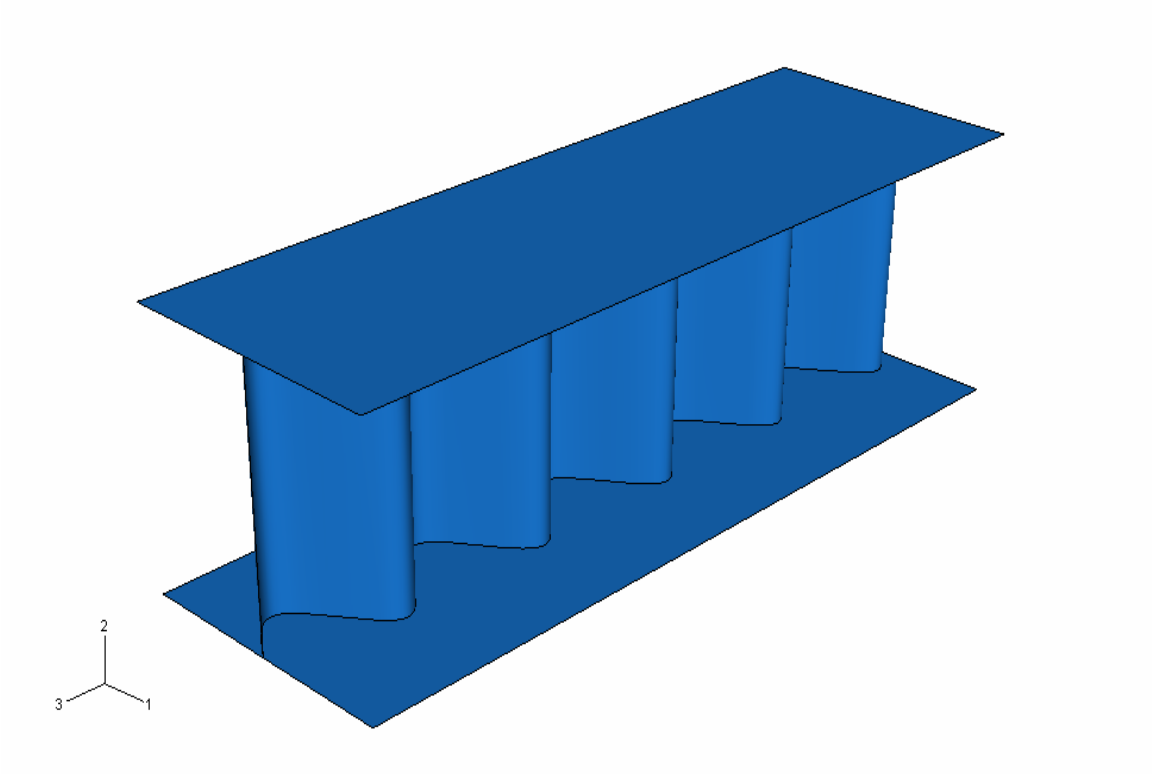

Figure 2.1.1: Geometry of Sine Wave Beam Having Five Periods and Web Amplitude of Forty Millimeters

The previous work into axially crushed energy absorbers focused on closed section structures, specifically tubes. Since there was little mention of open section absorbers, the idea was raised to investigate them. The sine wave beam was chosen out

of the various types of open sections based on the hypothesis that the shape of the web will dictate the deformation of the upper and lower plates and allow the crushing of the beam to progress in a predictable and repeatable manner. The sine wave beam has been studied quite extensively under the conditions of lateral impact, such as a helicopter sub-floor structure (Farley 1992). However, its geometry had not yet been explored under an application of axial impact. The introduction of the sine wave shape to the web of the beam should induce fold lines across the width of the upper and lower plates at prescribed positions, in order to control the crushing mechanism. Theoretically, the plate will have peak buckle deformations at the minimum and maximum points of each sine wave period. The dashed lines in Figure 2.1.2 illustrate these peak locations. This "controlled" buckling mode is the premise behind this thesis and is referred to hereafter as the prescribed buckling mode.

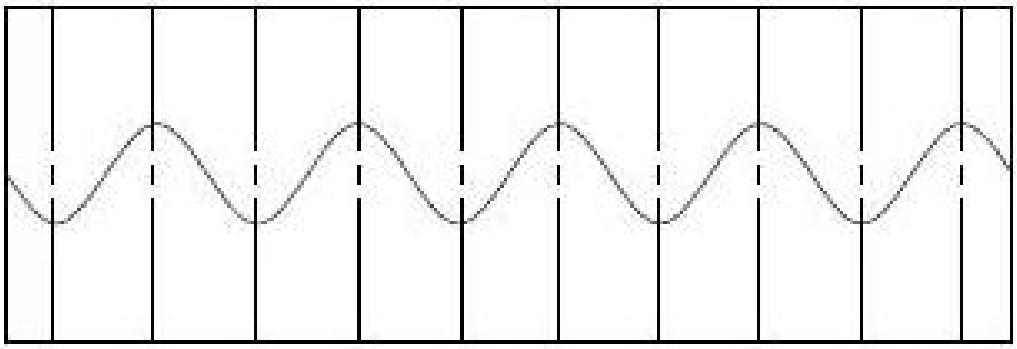

Figure 2.1.2: Illustration of Induced Folding Pattern in Relation to Beam Web Geometry.

This approach differs from the prismatic structures since the folding should take place at each of these lines regardless of the remaining beam dimensions. Figure 2.1.3 shows the lowest eigenmode of deformation in the upper and lower plates, which results from a

linear buckling analysis on the structure. This analysis will be explained in depth in the following section describing the computational model.

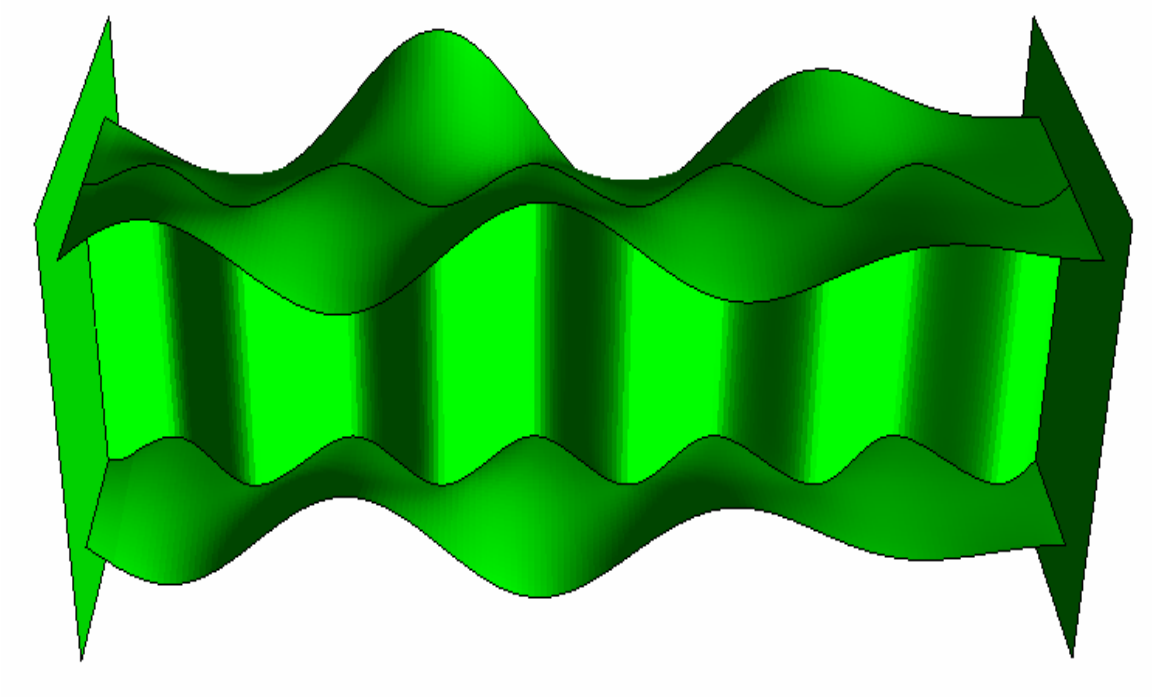

Figure 2.1.3: Lowest Eigenmode of Deformation

During the crushing process, energy is absorbed through the plastic deformation of the upper and lower plates. The manner in which this deformation takes place depends on the geometry of the beam. That geometry has many variable parameters which are given as follows:

- Number of sine wave periods along length of beam
- Amplitude of sine wave web
- Thickness of upper and lower plates
- Thickness of sine wave web
- Height of web vs. length of beam
- Width of upper and lower plates vs. length of beam

- Height of web vs. width of upper and lower plates
- Beam material
- Web shape, e.g. sinusoidal, corrugated, non-periodic, etc.
- Upper and lower pate shape, e.g. rectangular, tapered, etc.
- Effect of a triggering mechanism on deformation behavior

This thesis focuses on four of these parameters: sine wave web amplitude, upper and lower plate thickness, web thickness, and number of sine wave periods along the length of the beam.

The beam has length, *L,* equal to 400 mm with width, *W*, and height, *H*, of 133.3 mm. The dimensional variables of the SWB are given in Figure 2.1.4. For all beam configurations other than the thickness study, a uniform thickness, *t*, of 1.5 millimeters is used.

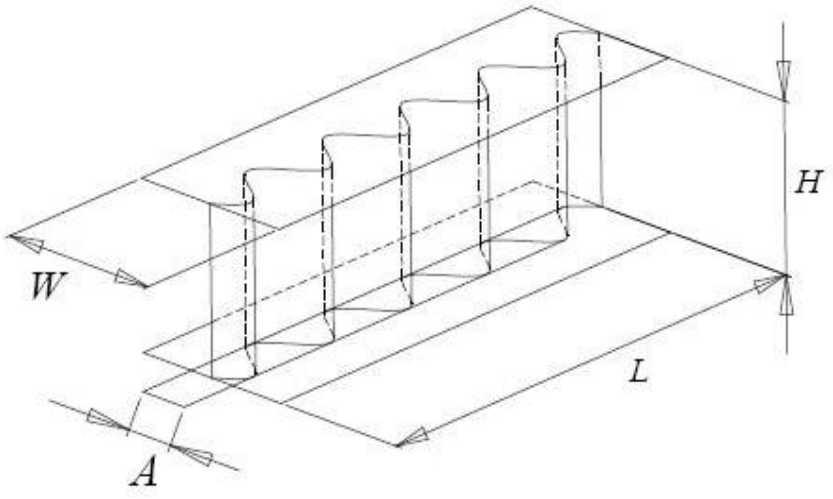

Figure 2.1.4: Geometric Dimensions of Sine Wave Beam

The web amplitude values, *A,* in Figure 2.1.4, used in the parametric study are 0 mm, 20 mm, 40 mm, 60 mm, and 80 mm. The numbers of periods investigated are 0, 2, 5, and 8. The thickness values used in the thickness study ranged from 1 mm to 3 mm in increments of 0.25 mm. The material was modeled as elastic-plastic mild steel. Its mechanical properties are density, ρ, of 7800 kilograms per cubic meter, yield strength, σ_y, of 304 MPa, Young's modulus, *E*, of 207 GPa, and Poisson's ratio, ν, of 0.3. To model a true crushing simulation, a plasticity model was created. The plasticity data was obtained from a tensile test performed by Nagel (2005) on a 2 millimeter thick specimen of mild steel. This material grade was chosen due to the similarity it has with the existing theoretical model for straight and double-tapered tubes (Abramowicz & Jones 1984; Reid & Reddy 1986). For more specific information on the method used to obtain the plasticity data see Nagel (2005). The values for the true stress and true plastic strain are given in Table 2.1.1.

Table 2.1.1: True Stress vs. Plastic Strain Material Data for Mild Steel.

σ_t (MPa)	ε_p (mm/mm)
304.6	0
344.19	0.0244
385.51	0.0485
424.88	0.0951
450.39	0.1384
470.28	0.1910

The strain rate effect that becomes important under dynamic loading was included in the material definition. The Cowper-Symonds constitutive equation, mentioned in the previous chapter, was used to account for strain rate. This material relation was utilized in the FE package by selecting the RATE DEPENDENT option in the material definition.

The two material parameters D, and q, equal 6844 s^{-1} and 3.91, respectively. These values were used in previous studies and account for the ultimate stress of steel specimens, making them applicable to large strain loading situations (Abramowicz & Jones 1984).

2.2 Computational Model Description

In order to develop an innovative geometry for energy absorption, an advanced FEA model was created with a commercially available package. To simulate the large deformation and self contact associated with axial crushing, the mathematical calculations require the use of a powerful suite of programs. The ABAQUS suite can be used for this model. It includes ABAQUS/CAE version 6.6, ABAQUS/Standard version 6.6, ABAQUS/Explicit version 6.6, and ABAQUS/Viewer version 6.6. Each of these programs was necessary to produce the final results for this loading condition.

2.2.1 Fundamentals of Finite Element Analysis

Finite element analysis has become an integral part of the design process for most structural or thermal applications. This tool can be used to predict the structural response of a given geometry under various loading conditions. Structural responses can be categorized into two categories, linear or nonlinear. A linear response means there is a linear relationship between the response of the structure and the load that is applied to that structure. A nonlinear response involves a part or assembly whose stiffness changes as a result of deformation. As all real world structures are actually nonlinear, a true linear analysis can only be used to approximate a structure's performance. The finite element analysis used in this thesis was nonlinear due to the nature of the structural response (Nagel 2005).

The structural response exhibited by the energy absorbers presented here is classified as nonlinear for two reasons: material nonlinearity, and geometric nonlinearity. The material model is nonlinear since the stiffness of the material changes when the stress exceeds the yield stress of the material. This results in plastic deformation of the geometry and altering of the structural integrity of the absorber. The response investigated here is also highly geometrically nonlinear due to the large deformation and self contact. These nonlinearities are addressed computationally by an incremental method of calculating the structural response. This type of computational method is referred to as the explicit method (Nagel 2005).

Two types of computational methods are used in finite element analysis, explicit and implicit. The implicit solving method is better suited for static, linear problems such as small displacements, and those that are only moderately nonlinear. Explicit analysis is better suited for loading cases such as high speed dynamics, complex contact between deformable bodies, complex postbuckling problems, and material degradation simulations. An explicit solver can typically take anywhere from 10,000 to 1,000,000 increments per simulation, but the computation required for each increment is relatively small. Considering this investigation involves both complex postbuckling and high speed dynamics, in addition to intricate contact with nonlinear materials, the use of an explicit solver was required (Hibbitt, Karlsson & Sorensen 2006).

2.2.2 Description of ABAQUS Program Suite

ABAQUS/CAE is the visually interactive environment that allows the user to pre- and postprocess each model. Preprocessing includes construction of the geometry, designation of material properties, application of the loading conditions, and the mesh

assignment. The user can run the simulation immediately or write the necessary input file to the hard drive to run later. Once the job is complete, the output file can be viewed in the Visualization module of CAE, ABAQUS/Viewer. In this module the user can see the output of the solver, and obtain all relevant output data. This data can then be exported to and external spreadsheet application for manipulation.

ABAQUS/Standard was used to execute an initial buckling analysis of each beam. This analysis was performed to help define reasonable initial imperfection shapes to introduce to the model. Previous work has shown incorporating these initial imperfections produces more accurate approximations of the crush deformation. These imperfections are explained further in the following section. ABAQUS/Explicit was used for the dynamic analysis and has proved to be a very powerful tool in crush simulations. The type of element assigned in the mesh is the same for implicit and explicit analyses. This element, designated S4R, has proved to be sufficiently accurate in previous crushing analyses performed by various authors (Nagel 2005). The element is a stress/displacement element capable of large strain deformation with integrated hourglass control. Hourglass control is necessary because of the reduced integration in the element's stiffness. Hourglassing is discussed further in Section 2.2.4.

2.2.3 Explanation of ABAQUS implementation

The beam geometry was created in ABAQUS/CAE with the geometric dimensions given in Section 2.1. Separate models were created for each parametric study involving web amplitude and period number. Only one model was created for the thickness study. Five parts were used in each SWB model, two rigid end plates, two flange plates, and the sinusoidally shaped web. The flange plates and web were modeled

as 3-D deformable, shell extrusions. The flange plates were located parallel to each other, with the web located perpendicularly between them. Using a tie constraint, the upper and lower plates were attached to the web, fixing the tangential displacements of connecting web nodes. The rigid end plates were modeled using one rigid element and a central reference point having point mass of 90 kg. One plate was fully fixed in space to simulate a rigid wall. The other was fixed in all directions but the axial, allowing it to translate along the crushing axis at a speed of 15 m/s. The translating plate represented the impacting body, which carries the kinetic energy causing the crush deformation of the absorber.

One end of the beam was rigidly attached to the translating plate with a tie constraint unlike the one previously mentioned. This tie simulated a cantilever attachment where the nodes at the end of the beam are fixed in all degrees of freedom. The opposing end of the beam was located with an initial gap of six millimeters to the other rigid plate. The nodes at this end of the beam were constrained in both tangential displacement directions, but allowed to rotate about all three axes. This simulated the impacting end of the beam locking into a grooved surface. This boundary condition was applied to keep the focus of the test on the crush deformation of the absorber instead of the intricacies of the surface interaction between beam and plate. This boundary condition is valid under the assumption that the absorber acts as part of an overall structure, like a supporting structure inside a car bumper. For consistency all other structures were subjected to this condition. The length of the crushing analysis was set to three hundredths of a second. This length was deemed appropriate since each absorber

either fully absorbed the initial kinetic energy, or experienced compaction to the point of the rigid end plates contacting each other.

The initial buckling analysis was performed to calculate the eigenmodes of the structure used for the initial imperfections. The result of the buckling analysis was output as a node file that was introduced into the dynamic model using the *IMPERFECTION keyword in ABAQUS/Explicit. Since the velocity of the impact was relatively low in speed, i.e., non-ballistic, the analysis required only the first ten buckling modes. Had the impact been a ballistic or blast type impact, a much larger number of buckling modes would have been required to accurately predict the necessary initial imperfections. For each eigenmode, the maximum deformation value calculated during the linear buckling analysis is scaled automatically by ABAQUS/Standard to 1.0 m. ABAQUS recommends that this value should be scaled down so that the maximum imperfection is on the order of 2% of the shell thickness. For this analysis, a value of 2.0e-2 mm or 1.3% of the shell thickness was used for the first eigenmode. For the remaining eigenmodes, a decreasing scaling factor was used and these are given in Table 2.2.1. These values were chosen based on recommendations from the ABAQUS user's manuals.

Table 2.2.1: Initial Imperfection Factors.

Eigenmode	Imperfection factor (mm)	Percentage of thickness
1	2.0E-02	1.3%
2	8.0E-03	0.53%
3	4.0E-03	0.27%
4	1.8E-03	0.12%
5	1.6E-03	0.11%
6	1.0E-03	0.067%
7	1.0E-03	0.067%
8	8.0E-04	0.053%
9	2.0E-04	0.013%
10	2.0E-04	0.013%

The buckling modes for three of the geometries tested are featured in Figures 2.2.3, 2.2.4, and 2.2.5. Introducing initial imperfection into the undeformed geometry creates a model that more closely correlates to experimentally achieved results (Hibbitt, Karlsson & Sorensen 2006).

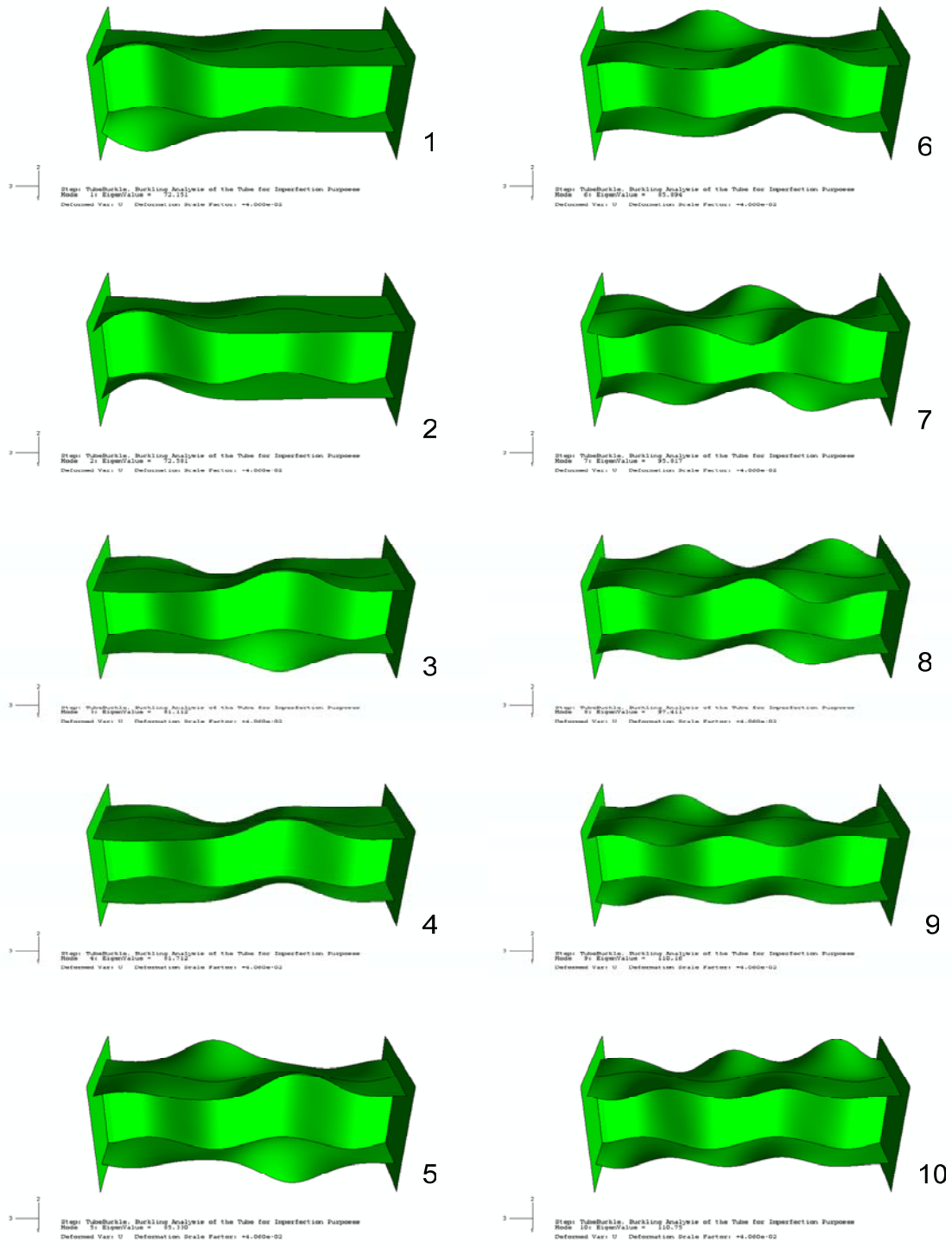

Figure 2.2.1: First Ten Eigenmodes Used for Initial Imperfections of Two-Period, Forty Millimeter Web Amplitude SWB.

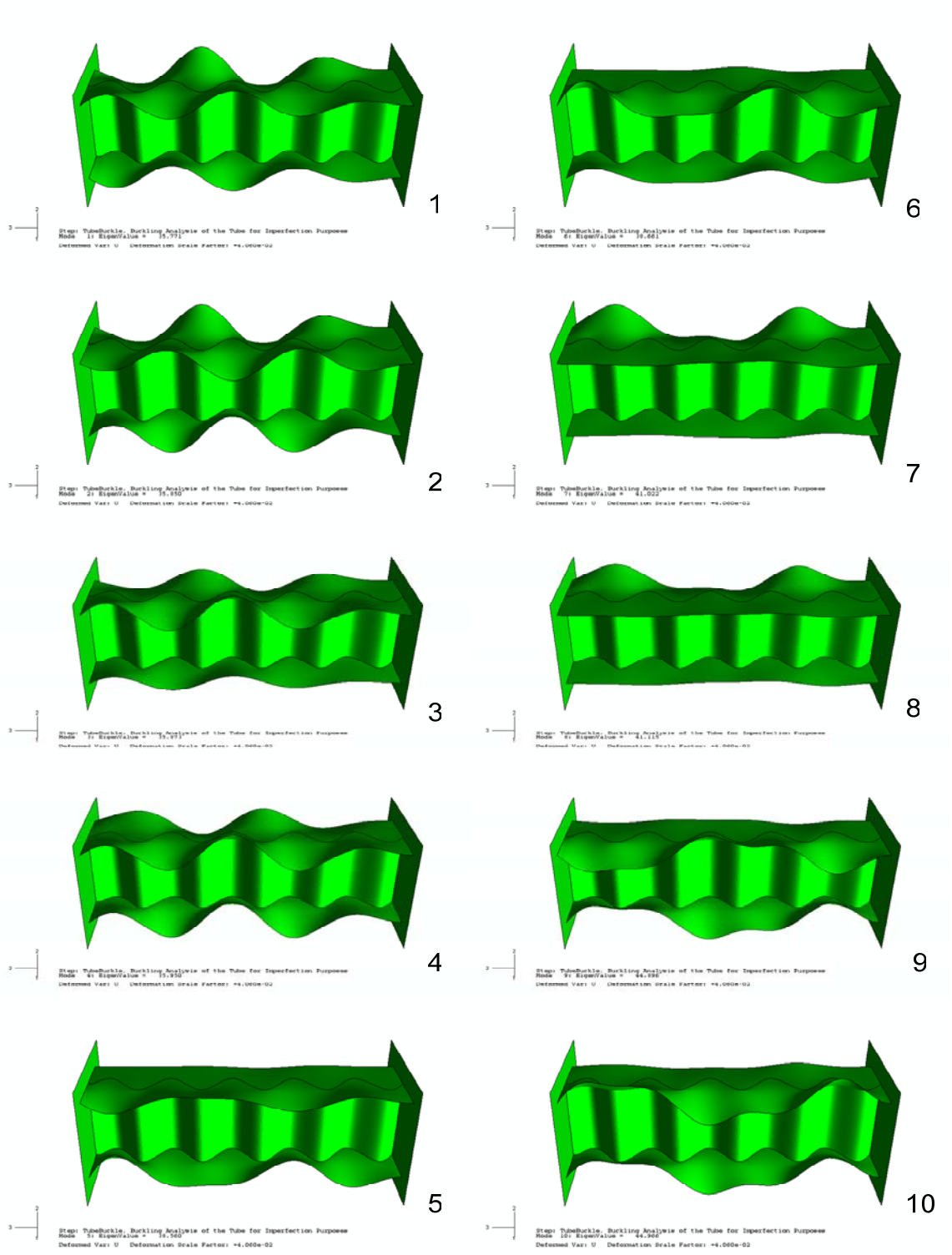

Figure 2.2.2: First Ten Eigenmodes Used for Initial Imperfections of Five Period, Forty Millimeter Web Amplitude SWB.

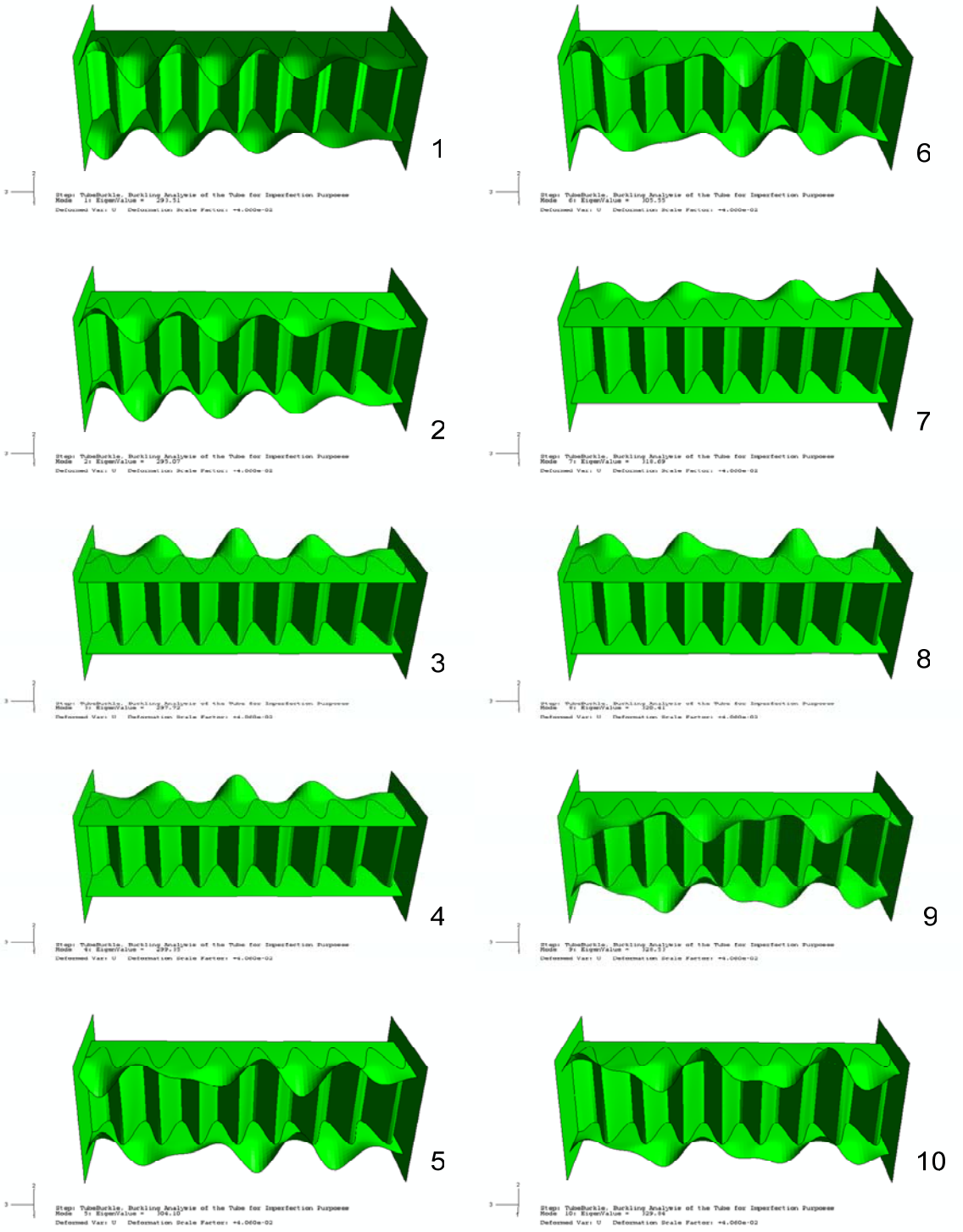

Figure 2.2.3: First Ten Eigenmodes Used for Initial Imperfections of Eight Period, Eighty Millimeter Web Amplitude SWB

2.2.4 Validation of ABAQUS models, mesh refinement, hourglassing and convergence discussion

To create a legitimate finite element analysis model, validation must be performed. This process involved reproducing an existing, previously validated, finite element model, running it, and comparing the results to the ones previously obtained. This procedure proved successful and the next step was then taken. The output was then compared to a theoretical model of a tube with the same geometry. The model used for validation consisted of a rectangular tube with width 100 mm, height 50 mm, and length 300 mm. The tube's thickness was 1.5 mm, with impacting mass and velocity of 90 kg, and 15 m/s, respectively. The theoretical mean force, P_m, is calculated using Equation (2.2.1), originally proposed by Abramowicz and Jones (1986).

$$P_m / M_0 = 52.22(c/h)^{1/3} \tag{2.2.1}$$

where c is the width of the tube, h is the thickness, and M_0 is the fully plastic bending moment per unit length calculated using:

$$M_0 = \sigma_0 h^2 / 4 \tag{2.2.2}$$

In quasi-static calculations, σ_0 is the yield stress. In dynamic calculations, this value is the average of the material's yield and ultimate stresses. This modification incorporates strain-hardening effects into the force value. The dynamic mean crushing force and actual force responses of the validation analysis are given in Figures 2.2.4 and 2.2.5, respectively.

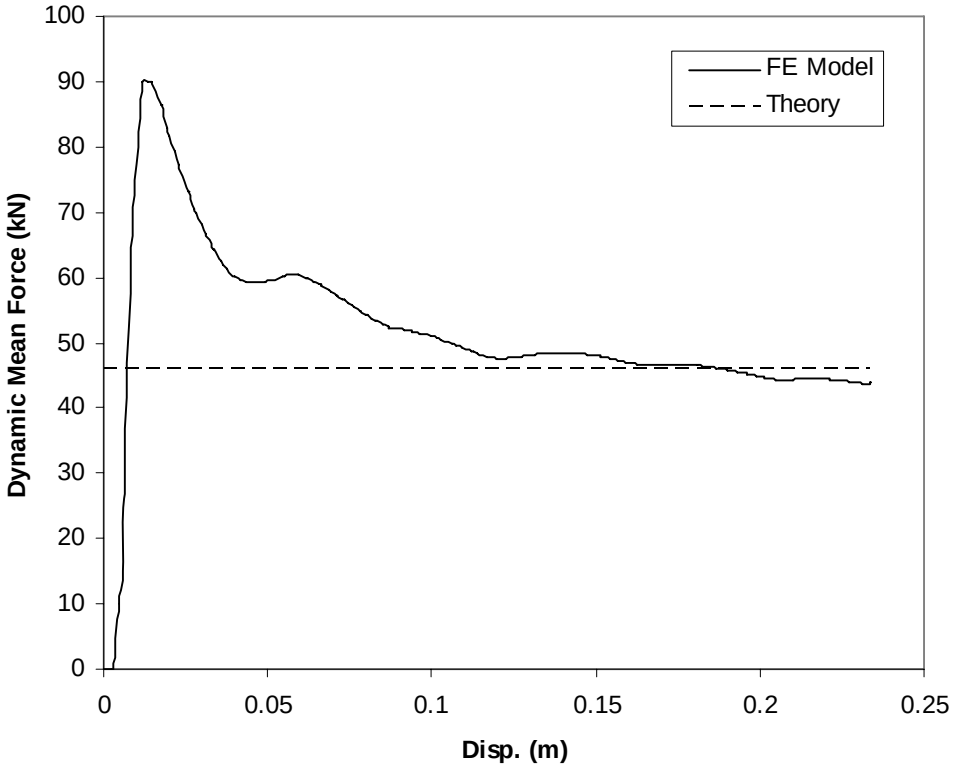

Figure 2.2.4: Dynamic Mean Force-Displacement Response with Theoretical Value for Validation of Crushing Analysis.

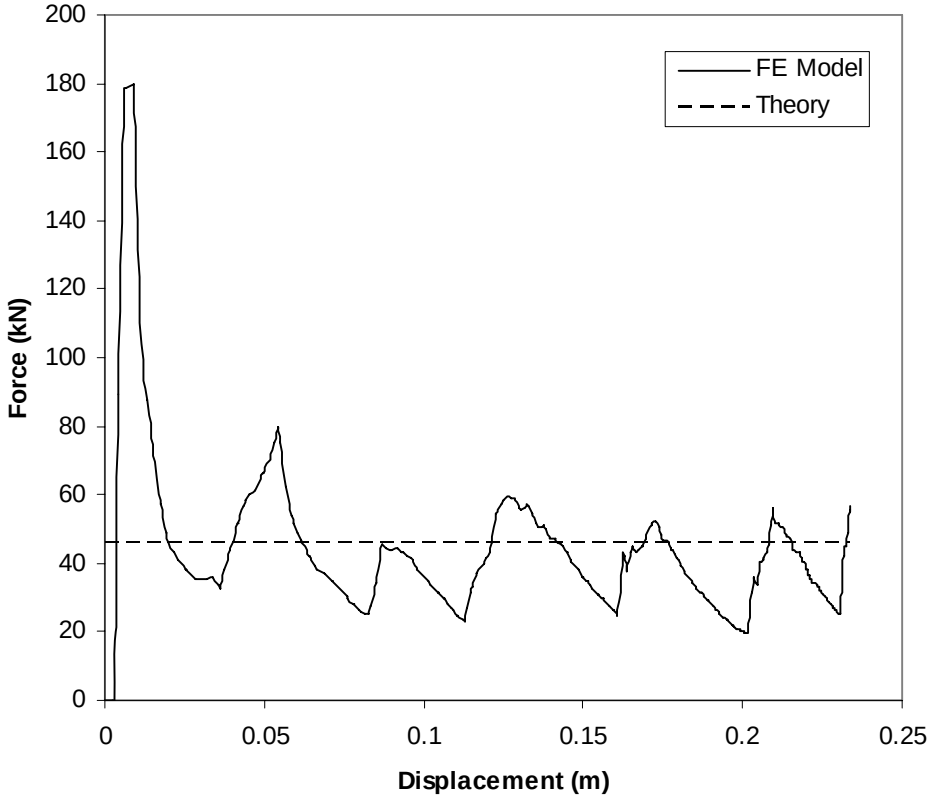

Figure 2.2.5: Dynamic Force-Displacement Response with Theoretical Value for Validation of Crushing Analysis.

As can be seen in the previous plots, the finite element model response approximates the theoretical value quite well. The remaining finite element models were modeled using the same boundary conditions, load, mesh size, and element type.

The mesh size found to produce convergence in the FE models was a square element of length 2.5 mm. A slightly larger element size would have been acceptable for convergence in the model. However, with any large deformation FE simulation the presence of hourglassing must also be investigated. Hourglassing is a zero-energy deformation mode where the nodes in the FE mesh translate from their original location,

but produce zero strain energy. This is not a rigid body motion and results from using a reduced integration element (Cook et al. 1989). Hibbett, et al. state this allowable limit, determined by taking the ratio of the artificial strain energy output (ALLAE) to the internal energy output (ALLIE), must remain below 5% for the entire simulation (Hibbett, Karlsson & Sorensen 2006). An element size larger than 2.5 mm resulted in ratios above the 5% limit. Figure 2.2.6 illustrates the time history response of the artificial to internal energy ratio of a 5mm element size plotted against the 2.5 mm.

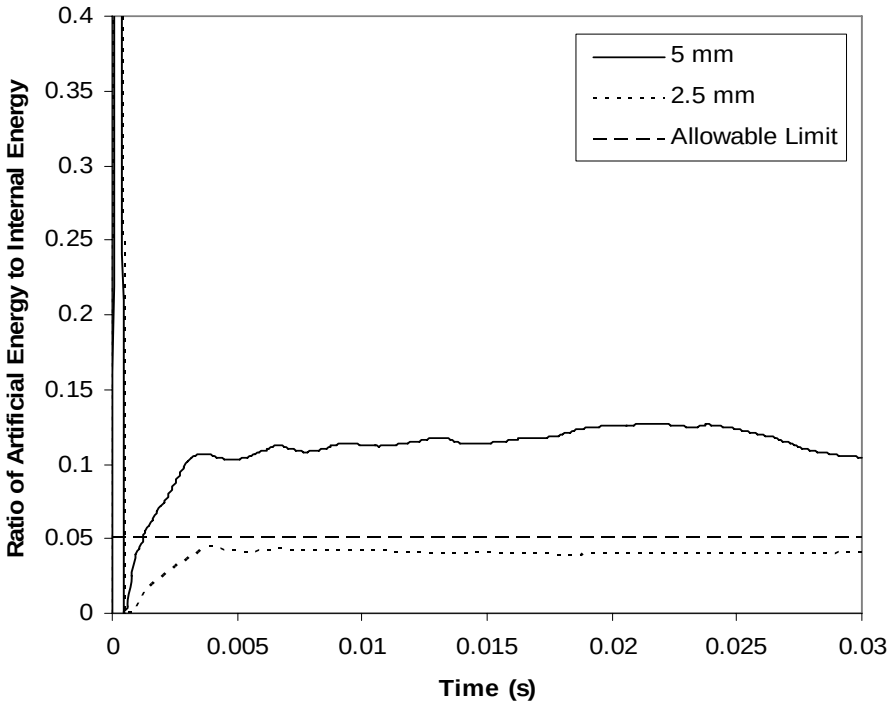

Figure 2.2.6: Time History Responses of Five Millimeter Element and Two Point Five Millimeter Element with Corresponding Allowable Limit Required by Literature.

The previous figure depicts the ratio of artificial energy to internal energy response of the validation model. As seen in the figure, the value for the 2.5 mm element stays below the allowable limit for the entire simulation, thus confirming this size as sufficient.

3. RESULTS

The energy absorbing characteristics for the sine wave beam (SWB) are similar to that of the prismatic structures. Introducing the sinusoidal shape to the web of the beam causes changes in the flange deformation during the crushing of the beam. The difference in this structure compared to the tubular or prismatic structures is the folding should take place at the prescribed location regardless of the beam's remaining geometric features. In prismatic structures, the thickness, width, and length ratios are the governing geometric factors in the deformation mode of the beam. In the SWB, the deformation of the beam is less dependent on the thickness, length, and width of the structure, and more dependent on the shape of the web. This should allow greater flexibility in manufacturing of the SWB as an energy absorber. The effects of variations in the geometric characteristics of the SWB are described in the following sections.

3.1 Effect of Thickness on Beam Having Five Periods and Web Amplitude of Forty Millimeters

Differences in geometric properties, such as thickness, can play an important role when investigating the energy absorbing performance of various structures. Nagel (2005) stated that for straight and tapered tubes, an increase in the wall thickness leads to an increase in the mean crushing force. An increase in the wall thickness leads to an increase in absorbed kinetic energy (Nagel 2005). In the SWB structures thickness was investigated on the model configuration with five periods and web amplitude of 40 millimeters. For this study, the thickness of the upper and lower flange plates and the

web was varied from one millimeter to three millimeters, in increments of one-quarter of a millimeter. Figure 3.1.1 shows that the resulting dynamic mean force increased as the thickness of the flange plates and web increased.

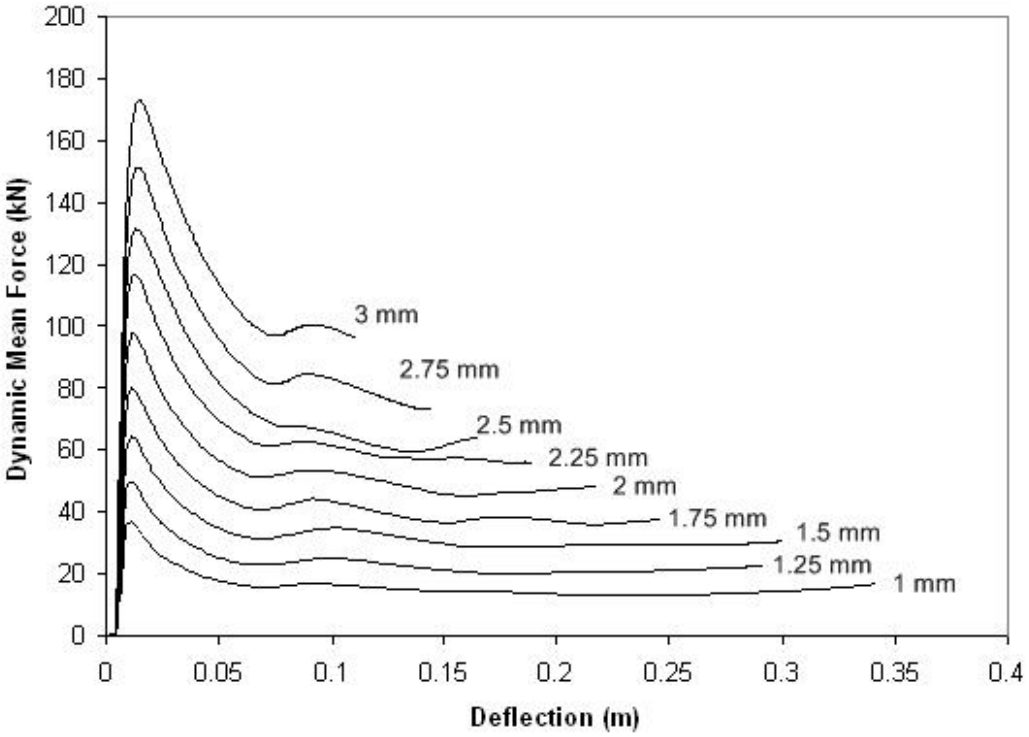

Figure 3.1.1: Effect of Wall Thickness on the Dynamic Mean Force of Beam Having Five Periods and Web Amplitude of Forty Millimeters.

The following figure, Figure 3.1.2, shows the increase in energy absorption with the increase in thickness.

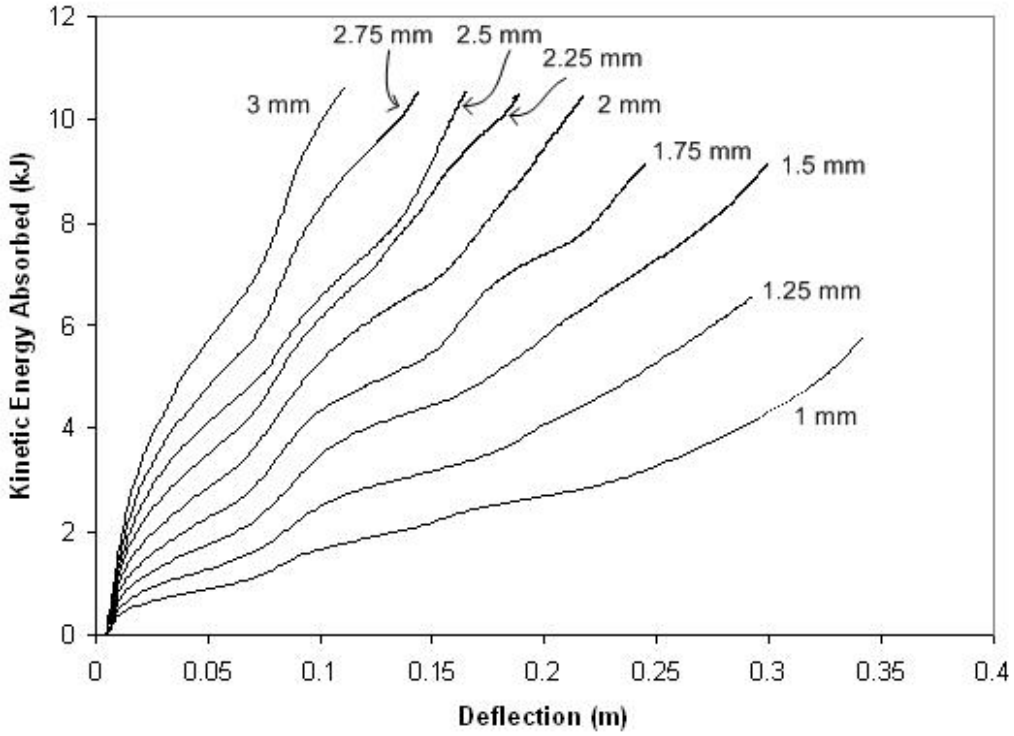

Figure 3.1.2: Effect of Wall Thickness on the Absorbed Kinetic Energy of Beam Having Five Periods and Web Amplitude of Forty Millimeters.

While the increase in thickness increases both the energy absorption and the dynamic mean force, there is another observed effect on the deformation of the structure. As the upper and lower flanges get thicker, the folding process during deformation becomes smoother and more predictable. Figures 3.1.3 and 3.1.4 illustrate the deformation of the one millimeter thick beam and the three millimeter thick beam, respectively.

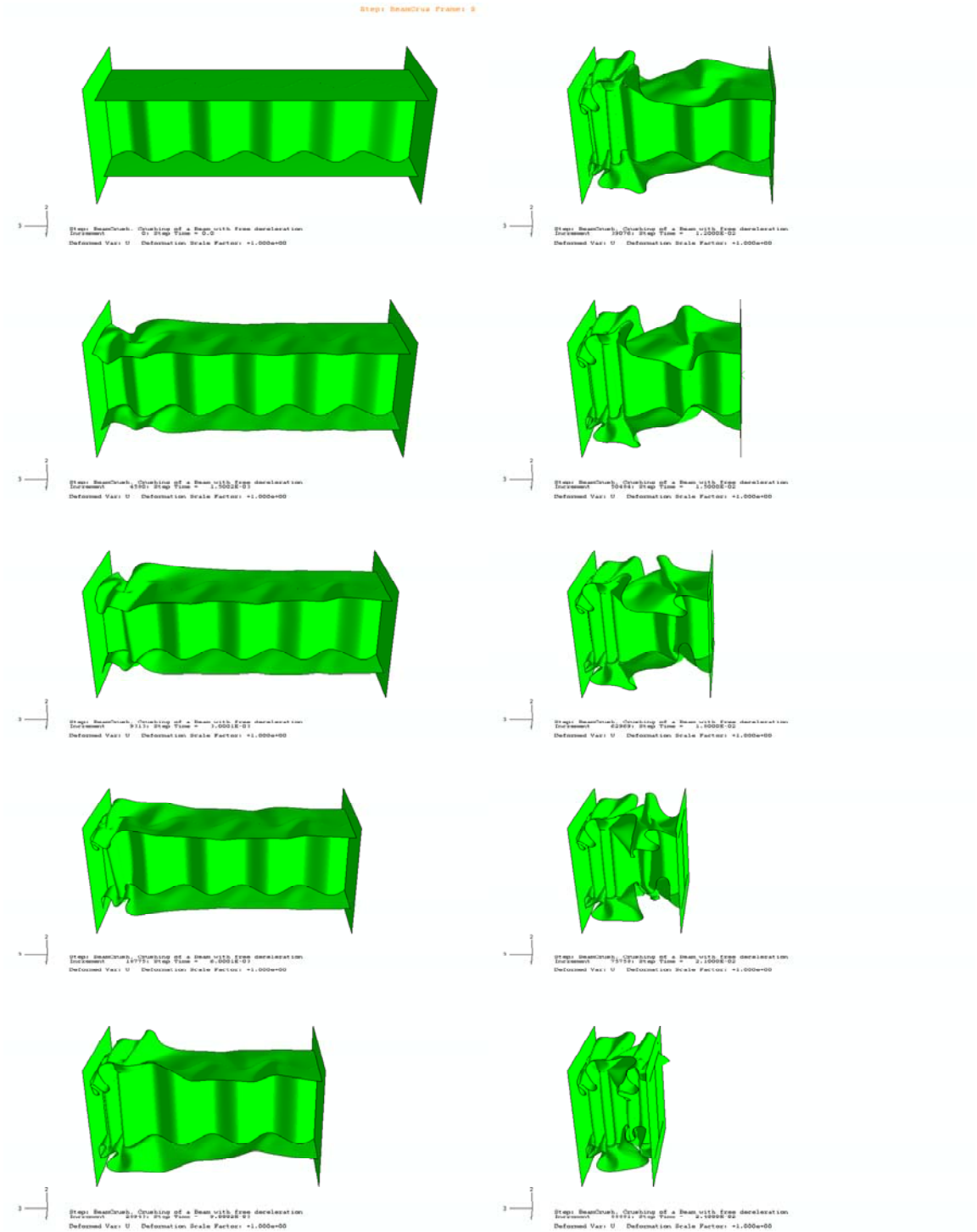

Figure 3.1.3: Axial Crush Progression of a SWB with Web Amplitude Forty Millimeters, Five Periods, and Thickness of One Millimeter.

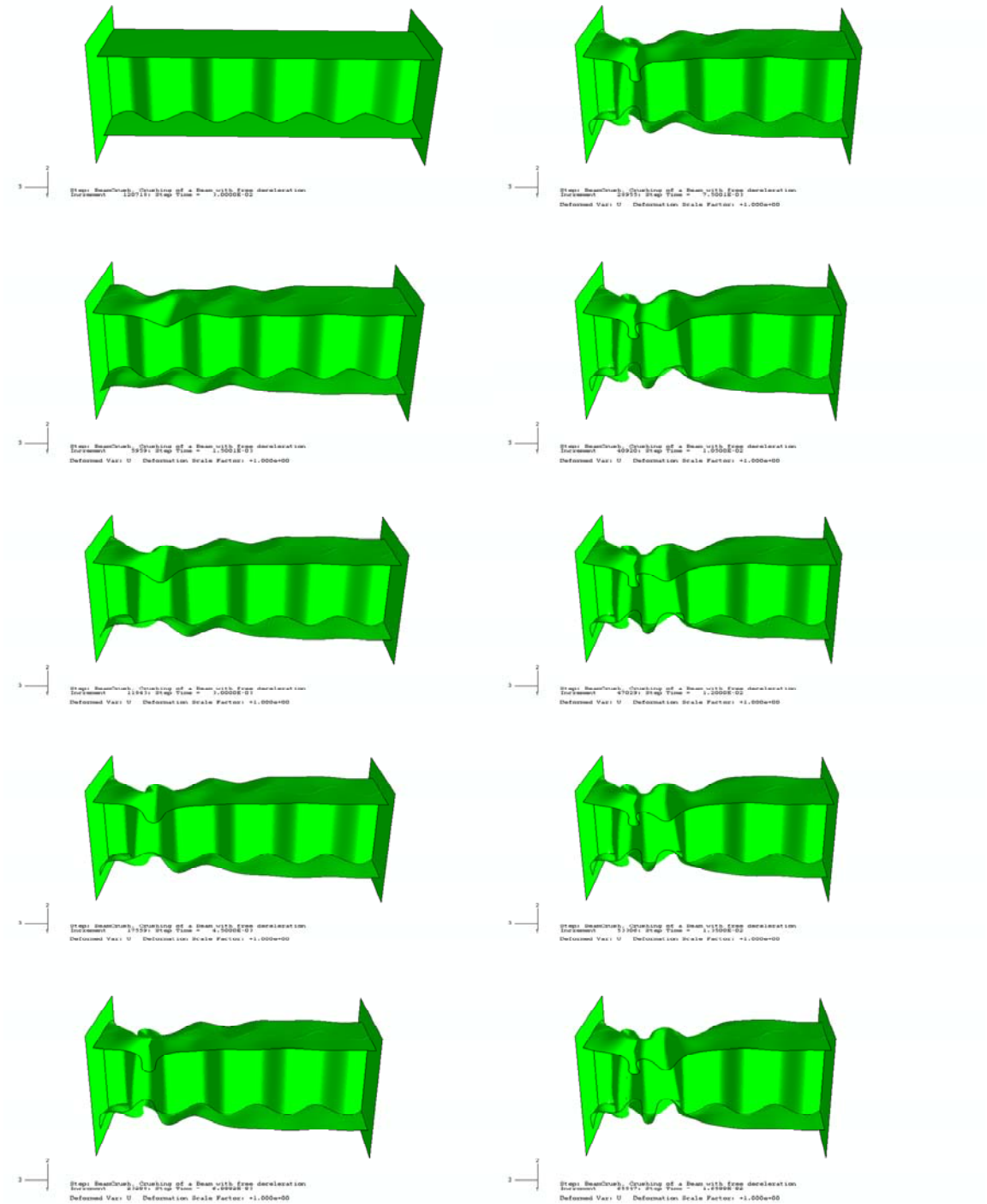

Figure 3.1.4: Axial Crush Progression of a SWB with Web Amplitude Forty Millimeters, Five Periods, and Thickness of Three Millimeters.

As shown in Figure 3.1.3 a large amount of wrinkling (local deformation) with deeper, more pronounced folding is experienced with the thinner beam elements. The upper and lower flange plates fold more easily but less predictably, requiring less bending moment to cause plastic deformation. The plastic stress wave propagation is also more detrimental with thinner flanges since there is visible deformation found in them after the wave has propagated along the beam. As the material becomes thicker, the wrinkling decreases and the folds in the flanges become shallower. This causes the structure to deform in a more prescribed manner. Thicker flanges require more energy to fold than thinner ones of equal length and width, therefore the folding mechanism is less severe and more predictable. Another observation from the previous two figures is that the stroke of the thicker beam is much shorter than the first. The thicker beam absorbs more energy per unit length and therefore requires a shorter stroke to absorb a similar amount of energy. There are advantages and disadvantages to this decrease in stroke length. Absorbing more energy per unit length is advantageous if the length of the absorber is constrained. This can be seen as a disadvantage also since with the force experienced by the impacting body is greater, resulting in more severe decelerations.

3.2 Effect of Web Amplitude

The first sine wave specific geometric parameter investigated was the amplitude of the sine wave web. This was investigated using a uniform thickness of one and a half millimeters, and period numbers of two, five, and eight. The bases of comparison for each web amplitude are the dynamic mean force-deflection and energy absorption-deflection responses.

3.2.1 Web amplitude effect with two periods

The initial test was performed using two periods and web amplitudes of 20, 40, 60, and 80 millimeters. These models are depicted in Figure 3.2.1 where the difference in web amplitude can be seen.

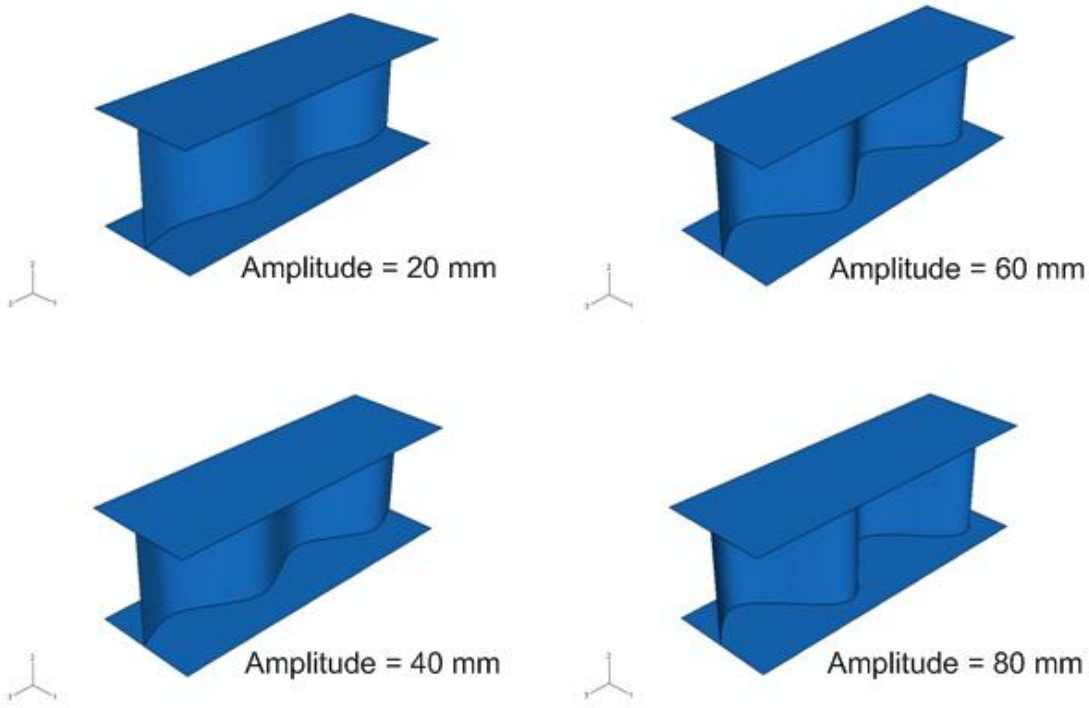

Figure 3.2.1: Sine Wave Beam Geometries Having Various Web Amplitudes, Two Periods, and Thickness of 1.5 Millimeters.

The dynamic mean crushing force-deflection response as a function of web amplitude is given in Figure 3.2.2.

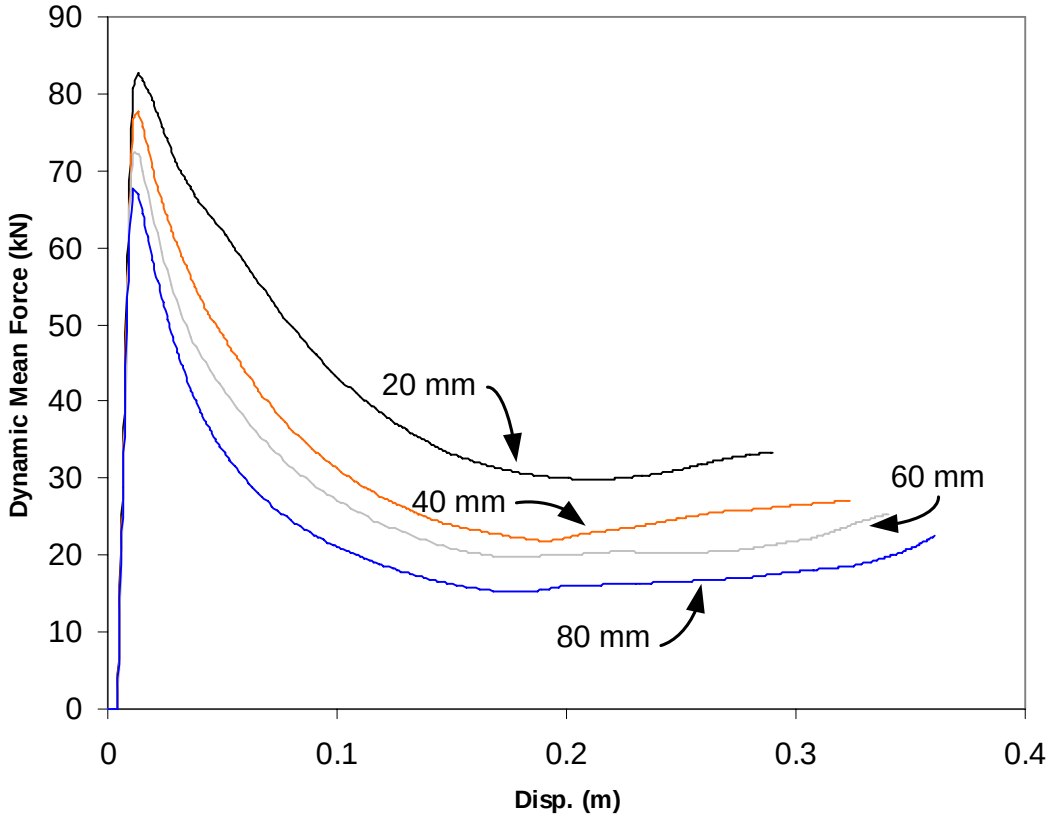

Figure 3.2.2: Dynamic Mean Force Versus Deflection for Two Periods with Varying Web Amplitude

As can be seen in the previous figure, web amplitude has a significant effect on the dynamic mean force response. This in turn affects the energy absorption, shown in Figure 3.2.3.

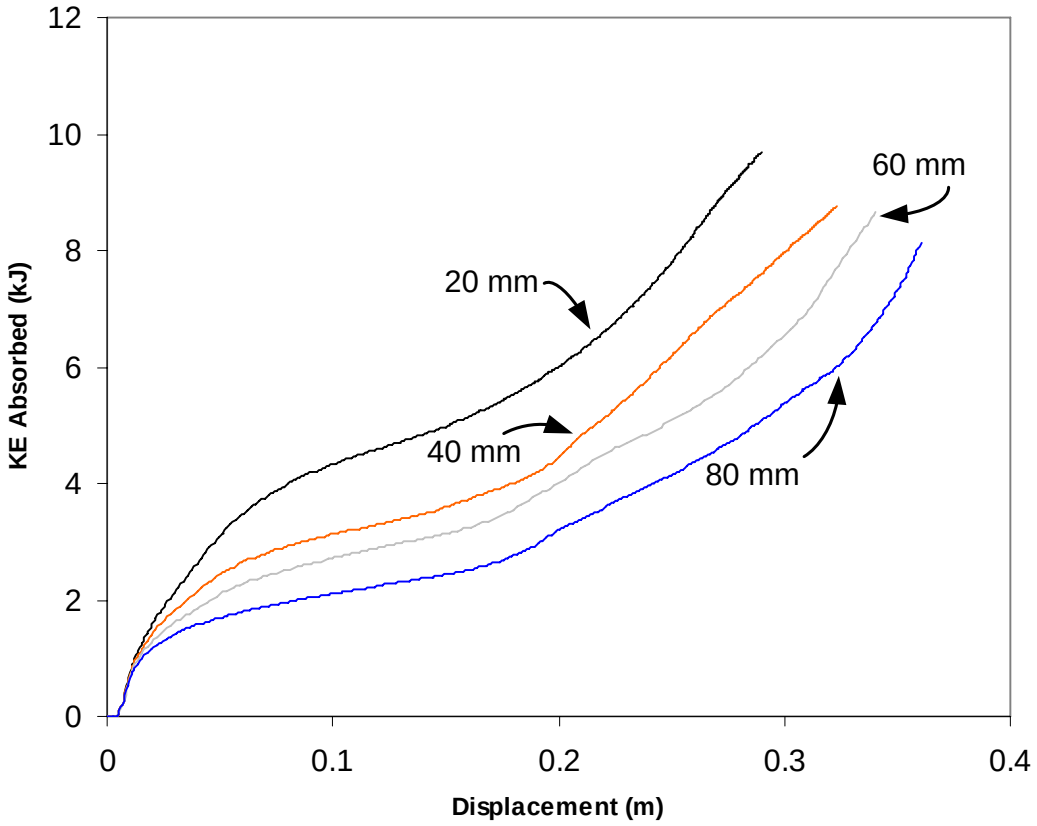

Figure 3.2.3: Absorbed Kinetic Energy Versus Deflection for Two Periods with Varying Web Amplitude.

As the web amplitude increases, the energy absorption decreases. With two periods along the length, the upper and lower flanges form four fold lines across their widths, one at each of the peaks and valleys associated with the sine wave. The crush progressions of the 20 mm and 80 mm web amplitude beams are given in Figures 3.2.4 and 3.2.5, respectively.

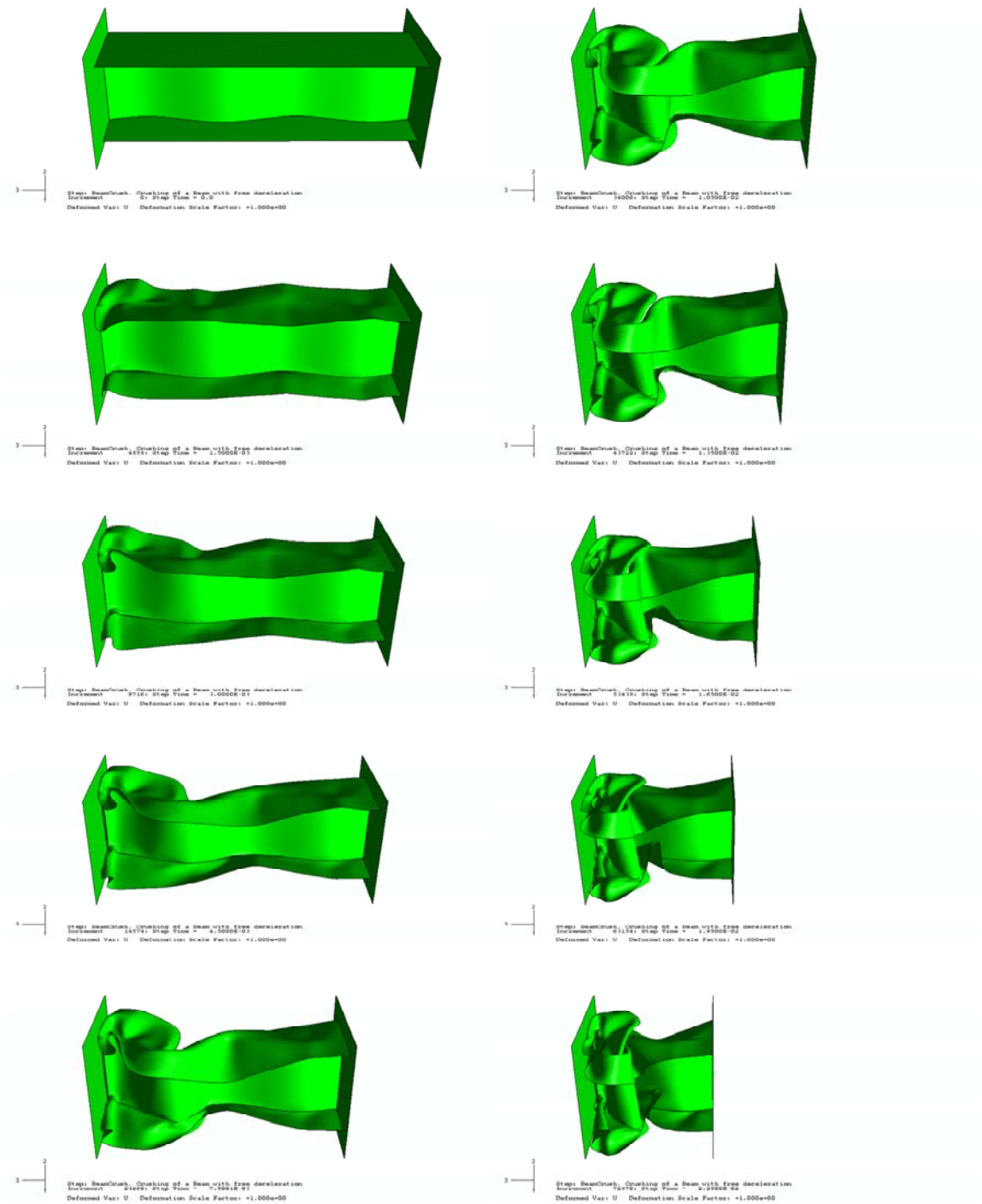

Figure 3.2.4: Axial Crush Progression of a SWB with Web Amplitude Twenty Millimeters, Two Periods, and Thickness of 1.5 Millimeters.

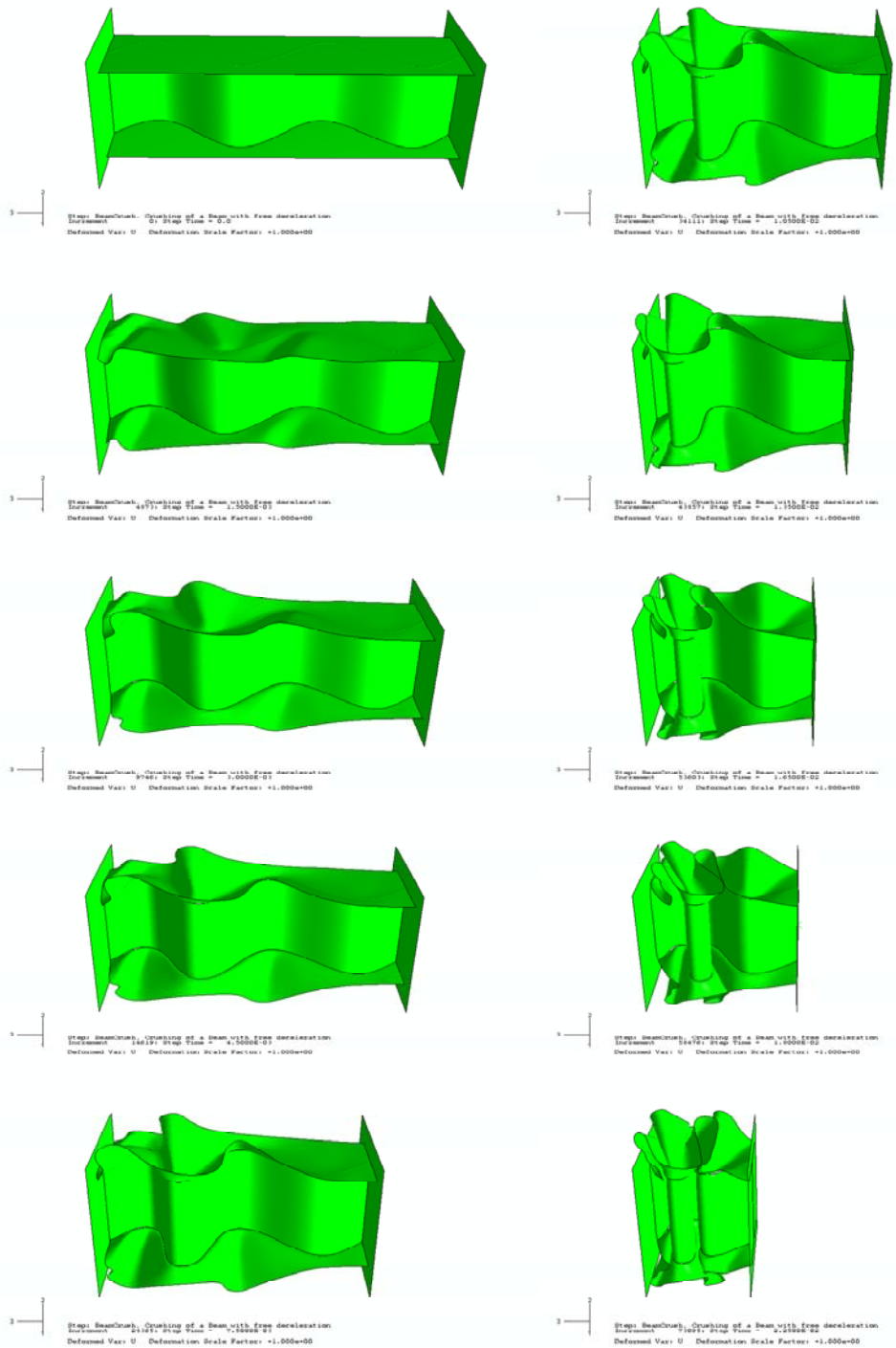

Figure 3.2.5: Axial Crush Progression of a SWB with Web Amplitude Eighty Millimeters, Two Periods, and Thickness of 1.5 Millimeters.

With an increased web amplitude, an increase in weight occurs due to the extra material present. The total mass of the 20 mm beam is 1.89 kg, where the 80 mm beam has a mass of 2.08 kg. For two periods, the 10% increase in weight is not significant. However, as the number of periods increases, the percentage increase in weight from the 20 mm beam to the 80 mm beam becomes significant. This is discussed further in the following sections.

3.2.2 Web amplitude effect with five periods

The second investigation was performed using five periods with web amplitudes of 20, 40, 60, and 80 millimeters. These models are illustrated in Figure 3.3.6 where the variations in web width can be seen.

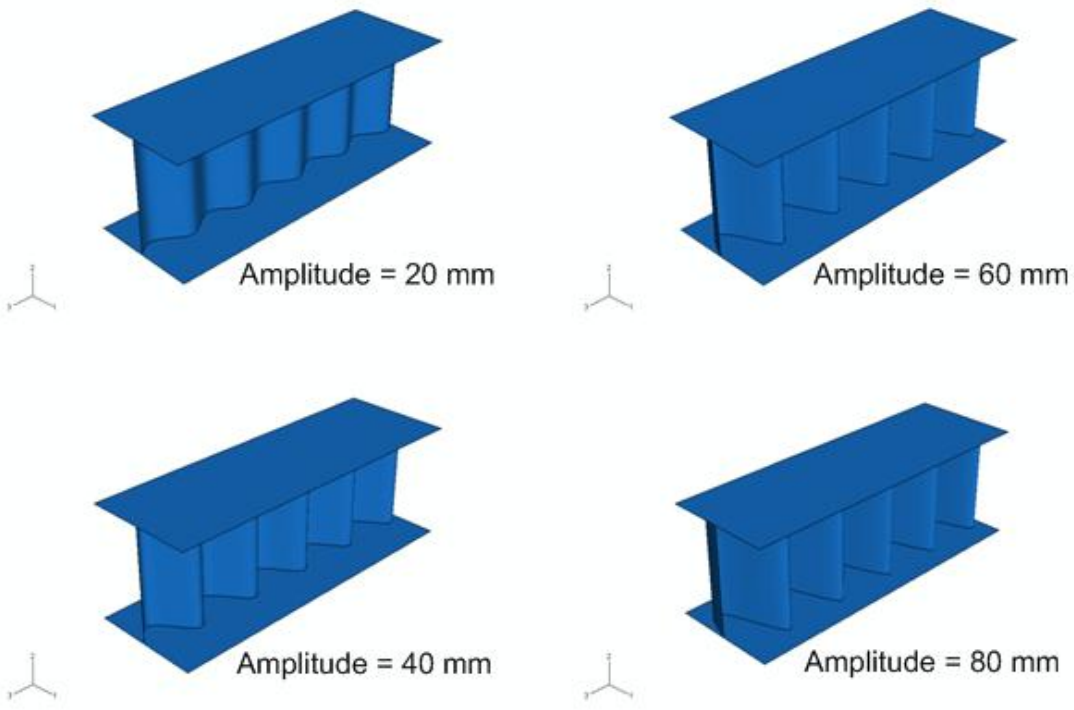

Figure 3.2.6: Sine Wave Beam Geometries Having Various Web Amplitudes, Five Periods, and Thickness of 1.5 Millimeters.

The mean force-deflection response is given in Figure 3.2.7.

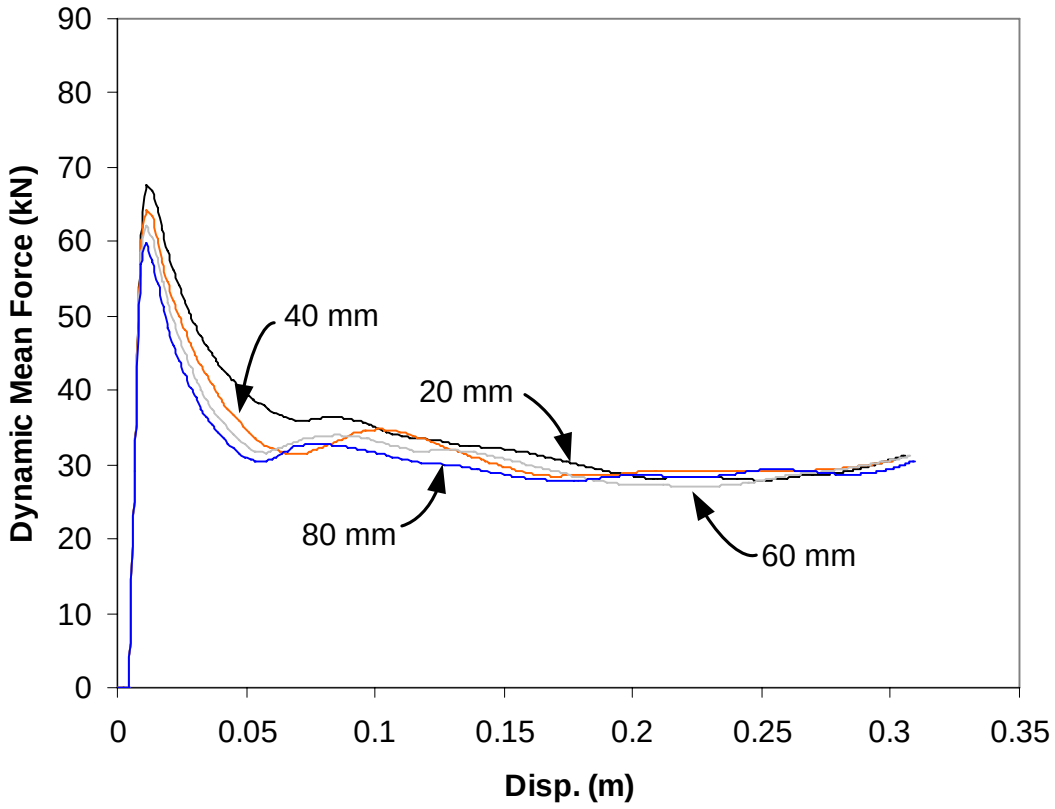

Figure 3.2.7: Dynamic Mean Force Versus Deflection for Five Periods with Varying Web Amplitude.

While the web amplitude has some initial effect on the dynamic mean force response, that effect diminishes altogether at an approximate crush distance of 0.175 meters. Prior to this point, the beam with the twenty millimeter web amplitude has the highest dynamic mean force and the eighty millimeter beam has the lowest. This effect of variations in web amplitude is however much smaller in the five period beam than in the two period beam.

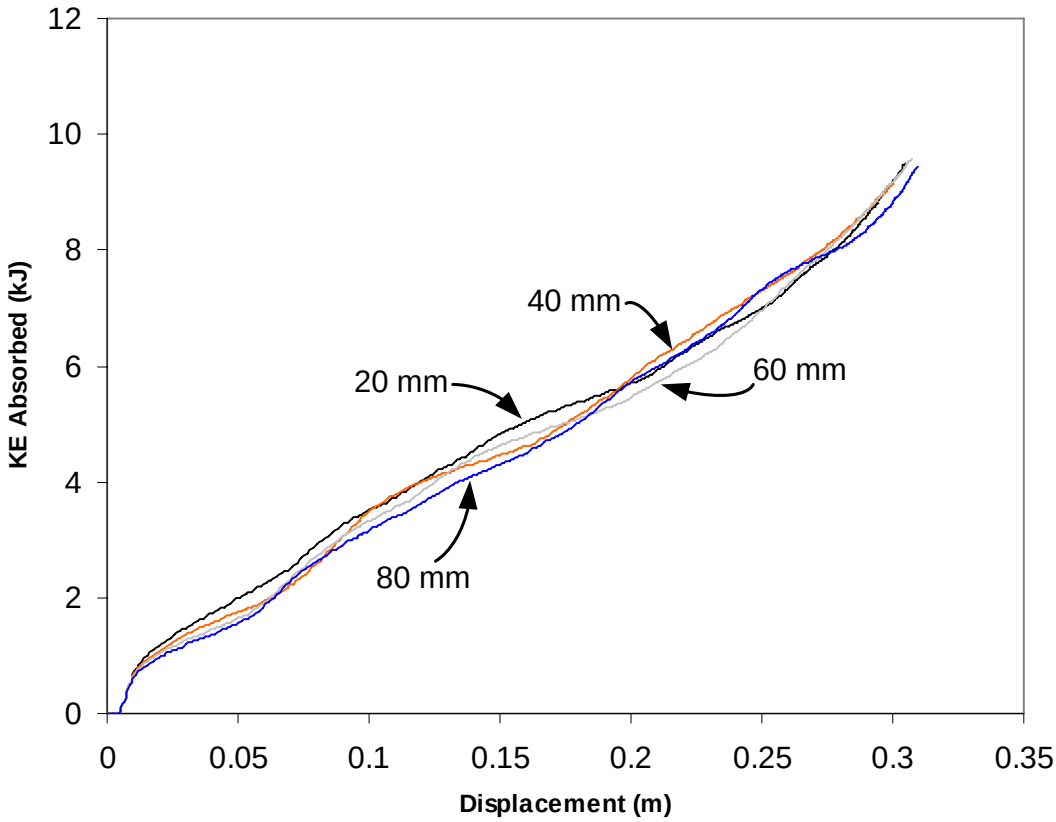

Figure 3.2.8: Absorbed Kinetic Energy Versus Deflection for Five Periods with Varying Web Amplitude.

Here it is apparent that for five periods, the web amplitude of the wave does not have a significant effect on the energy absorption of the beam. However, until the crush length reaches about 0.175 meters, the twenty millimeter web amplitude beam has slightly higher energy absorption, and the eighty millimeter has the lowest. This observation shows that during the initial crushing, the beam with the smaller amplitude is more efficient by absorbing more energy per unit length. Additionally, the smaller amplitude results in a reduction in weight. The energies absorbed per unit mass for the 20 mm web

amplitude versus the 80 mm web amplitude beam are 4.83 kJ/kg and 3.50 kJ/kg, respectively.

3.2.3 Web amplitude effect with eight periods

The third web amplitude test was performed on beams with eight periods. These geometries are illustrated in Figure 3.2.9.

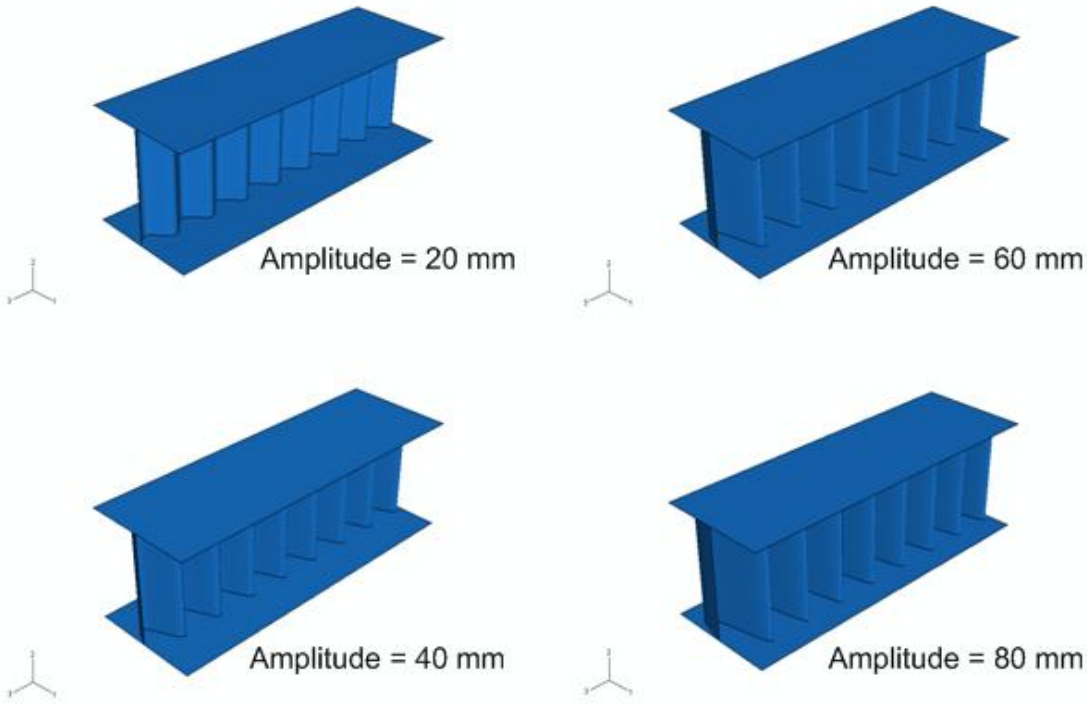

Figure 3.2.9: Sine Wave Beam Geometries Having Various Web Amplitudes, Eight Periods, and Thickness of 1.5 Millimeters.

The dynamic mean force-deflection response for each beam is given in Figure 3.2.10. As shown in the figure, upon reaching the crush length of 0.05 m the mean force is slightly higher in the 60 millimeter beam than the others. The other lines lie virtually on top of one another, showing the web amplitude has very little effect on the performance of the eight period beams.

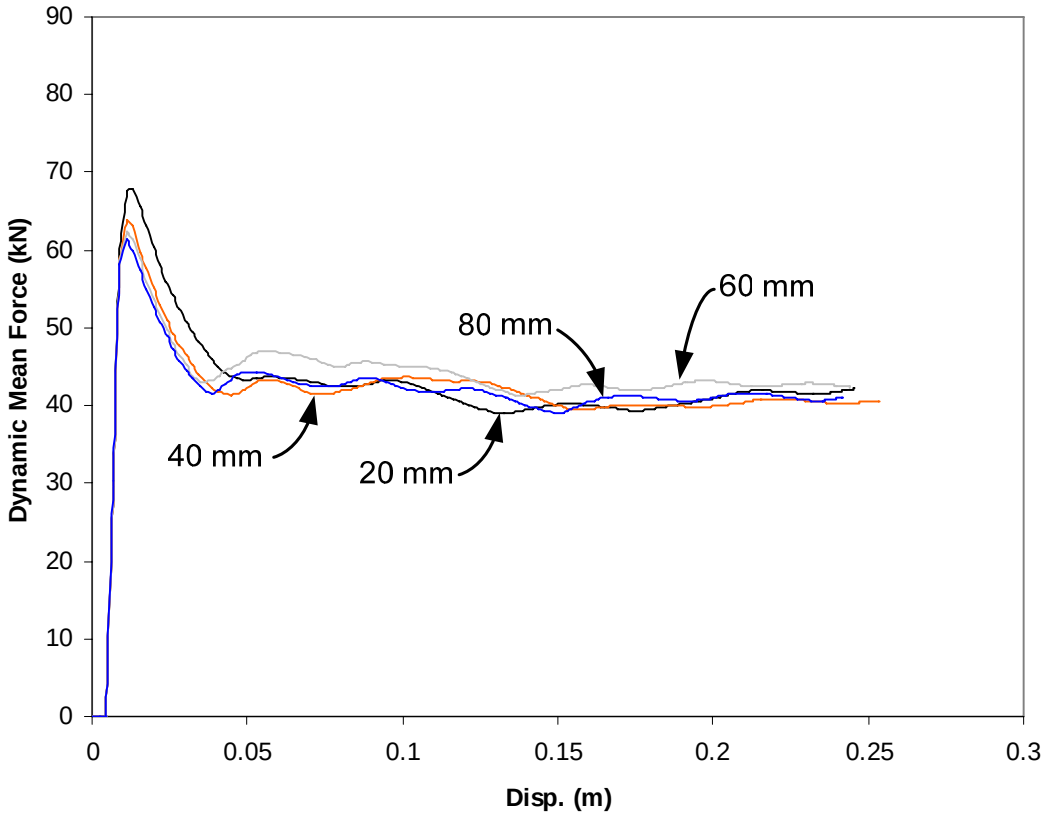

Figure 3.2.10: Dynamic Mean Force Versus Deflection for Eight Periods with Varying Web Amplitude.

Figure 3.2.11 shows the absorbed kinetic energy response of the beams. As in the previous figure, once the crush length surpasses 0.05 m the beam with web amplitude of 60 millimeters has higher energy absorption than the others. Except for this anomaly, the web amplitude has little effect on the eight period beams.

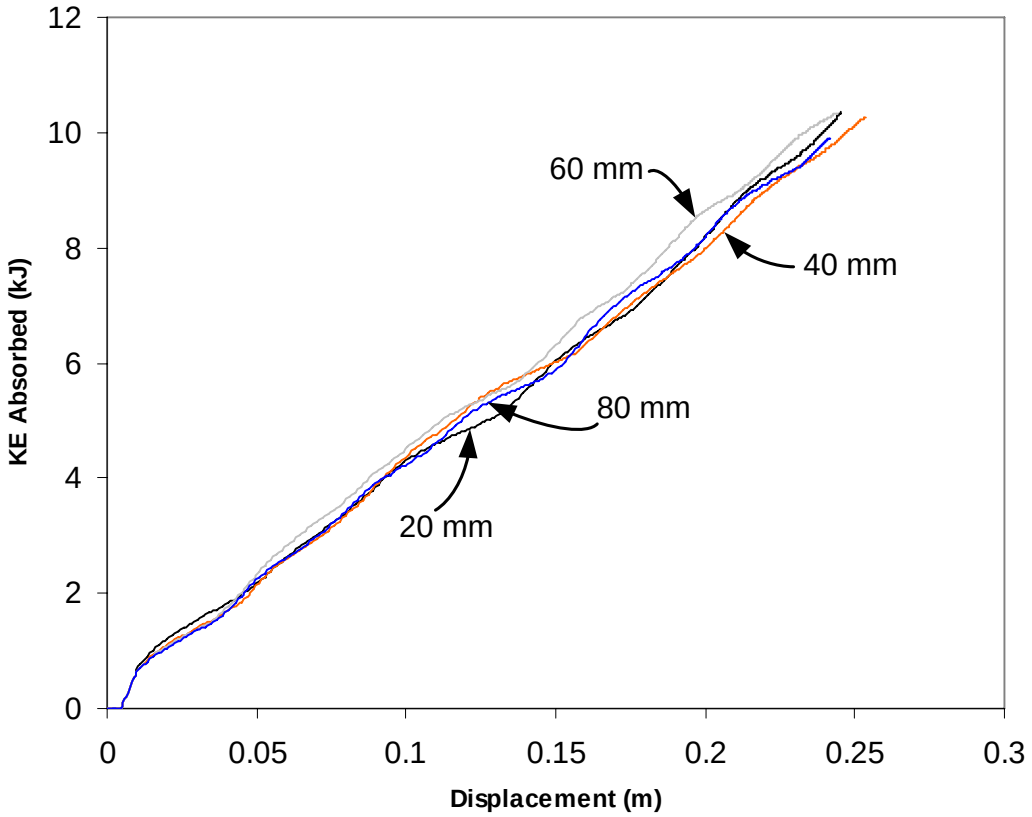

Figure 3.2.11: Absorbed Kinetic Energy Versus Deflection for Eight Periods with Varying Web Amplitude.

A few observations can be made with regard to the effect of web amplitude on the energy absorbing characteristics of the SWB. With a small number of periods, the web amplitude has a significant effect on energy absorption. Increasing the web amplitude decreases the energy absorption of the beam. However, once the number of periods reaches five or so, the effect of web amplitude diminishes greatly. Eventually with a high period number the web amplitude has essentially no effect on the energy absorption. A possible explanation for this is with high period number, other geometrical dimensions of the beam, thickness, height, and width, override the intended effects of the sinusoidally

shaped web. If this is indeed the case for these geometrical values, the optimal configuration of the eight period beam is of web amplitude 20 mm. Compared to the higher web amplitudes, the weight savings from material reduction are significant without any real decrease in performance. The energy absorbed per unit weight for the 20 mm web amplitude compared to the 80 mm web amplitude is 5.13 kJ/kg vs. 3.91 kJ/kg.

3.2.4 Observations as web amplitude approaches zero for two periods

As the amplitude of the web approaches zero, the SWB geometry approaches the geometry of an I-beam and therefore, the energy absorbing performance of the SWB approaches that of the I-beam structure. The following two figures illustrate how the dynamic mean force and absorbed kinetic energy responses of the sine wave beams approach the performance of the I-beam.

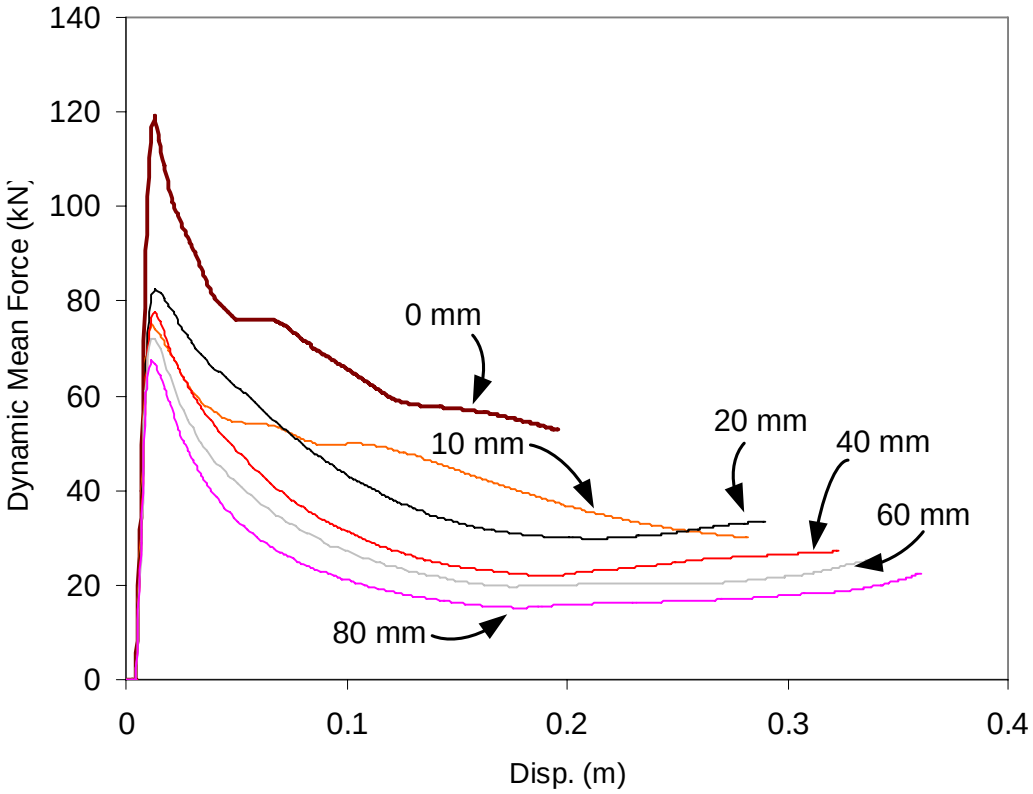

Figure 3.2.12: Dynamic mean force versus deflection for a SWB having two periods with varying web amplitude

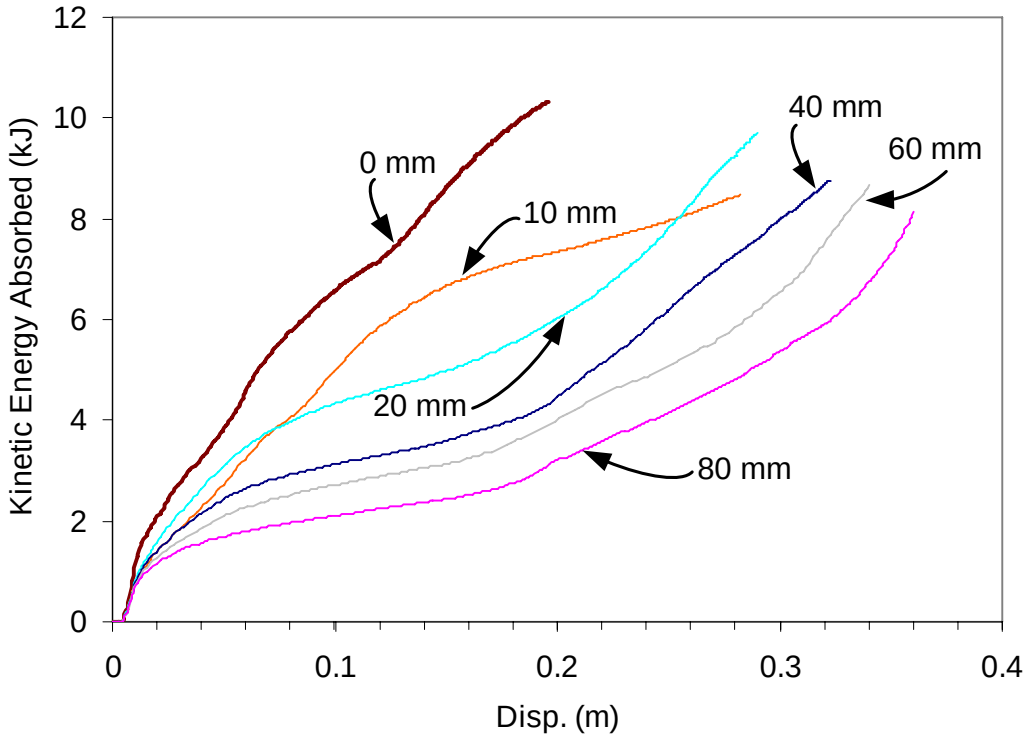

Figure 3.2.13: Absorbed Kinetic Energy Versus Deflection for Two Periods with Varying Web Amplitude.

These results indicate that the sine wave web has a direct effect on the energy absorbing performance of the beam. An additional web amplitude value of 10 mm was tested in this comparison to illustrate the convergence of the absorber's behavior with diminishing web amplitude. The dynamic mean force response line for this beam has a shape that is similar to the I-beam's response but with considerably less amplitude. After the initial peak, the I-beam's force drops sharply until the crush length reaches 0.05 m, where it briefly levels out, then declines for the remainder of the crushing process. The 10 mm line follows this same basic shape, but approximately 20 to 40 kN less in magnitude over

the entirety. This occurs because the web's amplitude was shallow enough for the structure to deform similar to the prismatic I-beam. In addition to the decrease in the dynamic mean force, a reduction in energy absorption per unit length is observed in Figure 3.2.13. The beams with 20 mm and larger web amplitude, experience a significant change in their energy absorption rates at crush length of 0.05 m. The same significant change in energy absorption rate for the 10 mm beam does not occur until the crush length reaches 0.125 m. This is the transitional point where the prescribed buckling mode becomes dominant over the localized wrinkling. Although there are transitional points found in the beams having five and eight periods, they are not as obvious as with the two period beams. The deformed shapes at the transitional points for the 10 mm, 20 mm, and 80 mm beams are illustrated in Figures 3.2.14, 3.2.15, and 3.2.16.

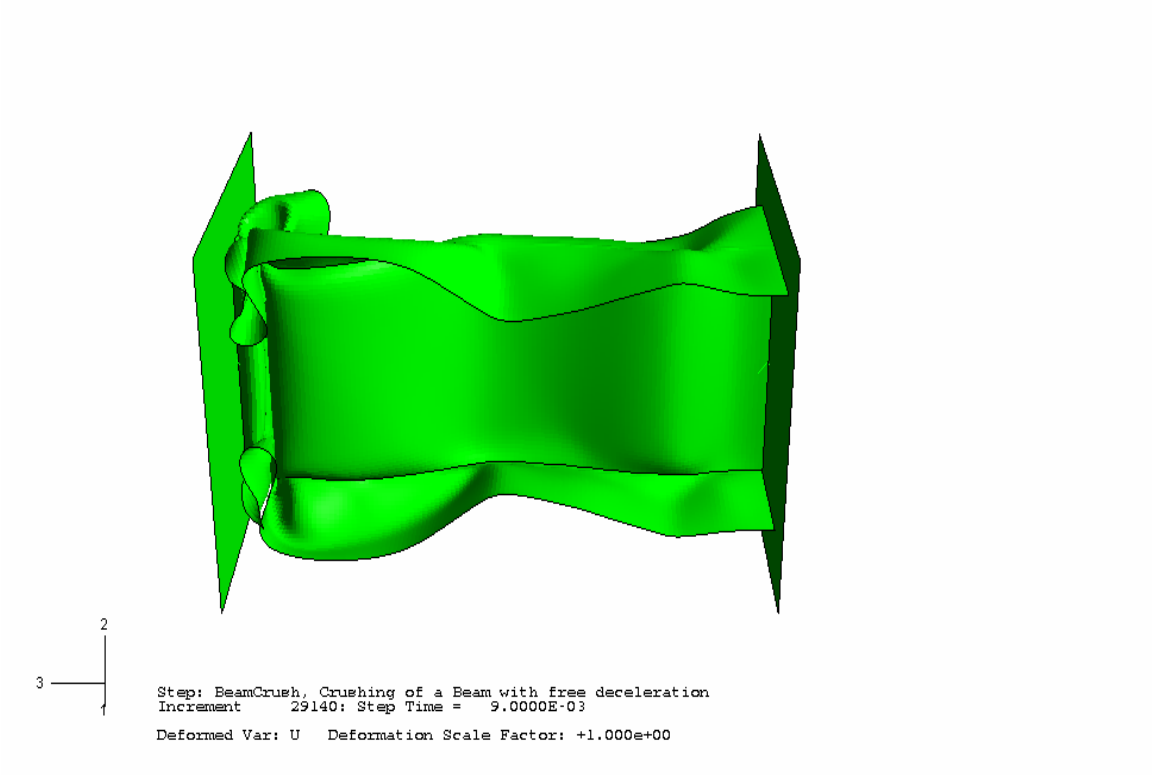

Figures 3.2.14: Deformed Shape at Transitional Point Where Prescribed Buckling Mode Becomes Dominant at Crush Distance of 0.0125 m for Two Period, Ten Millimeter Web Amplitude Beam.

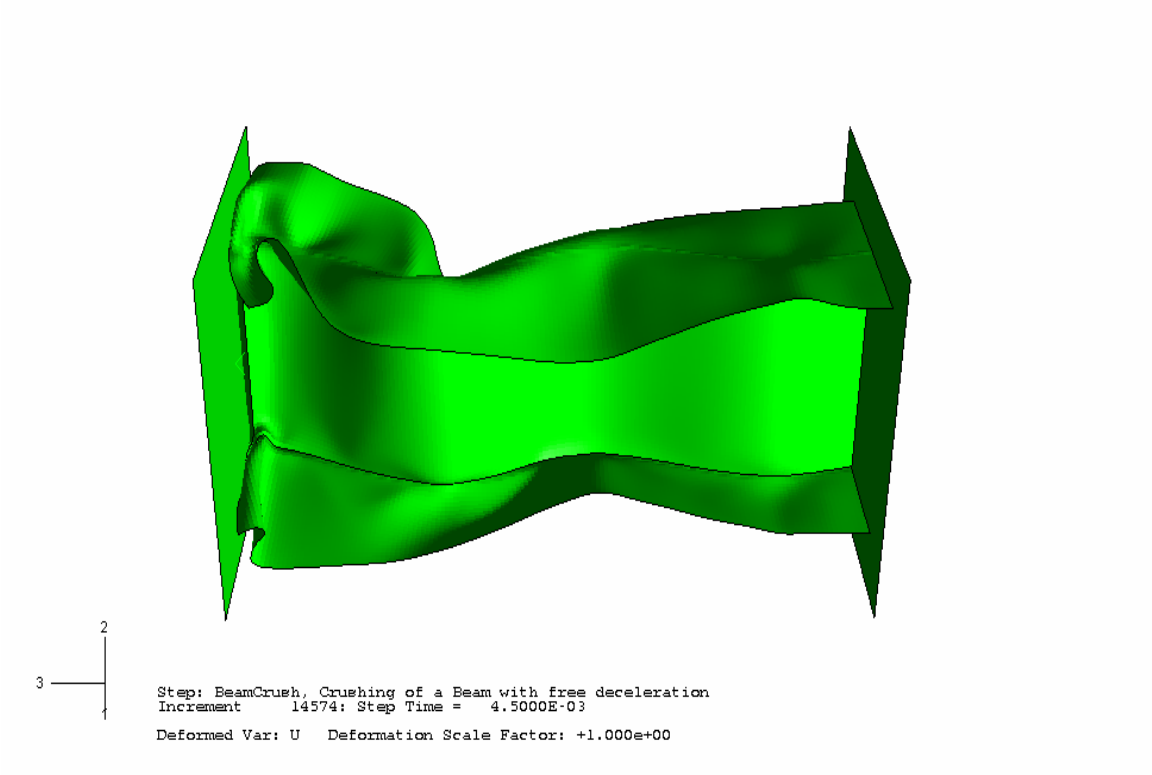

Figures 3.2.15: Deformed Shape at Transitional Point Where Prescribed Buckling Mode Becomes Dominant at Crush Distance of 0.02 m for Two Periods, Twenty Millimeter Web Amplitude Beam.

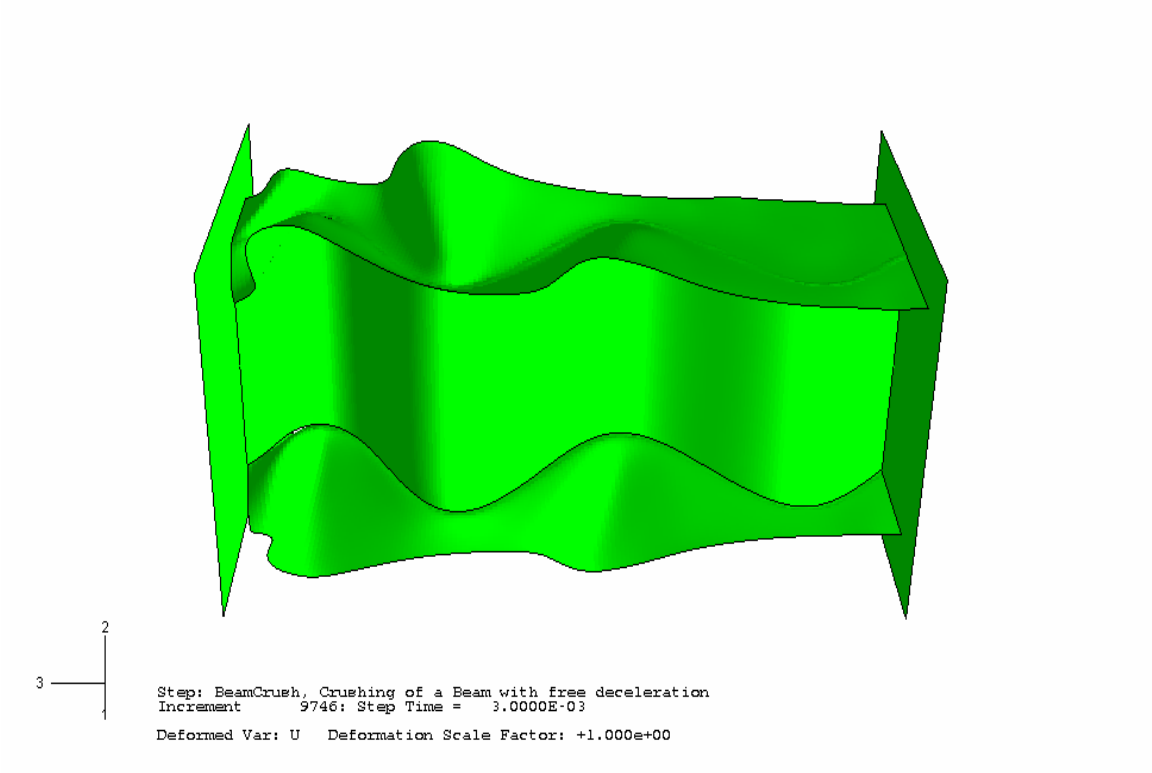

Figures 3.2.16: Deformed Shape at Transitional Point Where Prescribed Buckling Mode Becomes Dominant at Crush Distance of 0.02 m for Two Periods, Eighty Millimeter Web Amplitude Beam.

As the web amplitude increases, the prescribed buckling mode initiates earlier, decreasing the energy absorption and the dynamic mean force.

3.3 Effect of Period Number

The effect of period number on the energy absorbing performance of the SWB was studied using models with constant thickness of one and a half millimeters and web amplitudes of 20, 40, 60, and 80 millimeters. Again, the mean crushing force-deflection and energy absorption-deflection responses are the comparison criteria between the various studies.

3.3.1 Effect of period number with web amplitude of twenty millimeters

The initial investigation into the effect of period number was performed using two, five, and eight period beams with constant web amplitude of twenty millimeters. The beam geometries are depicted in Figure 3.3.1.

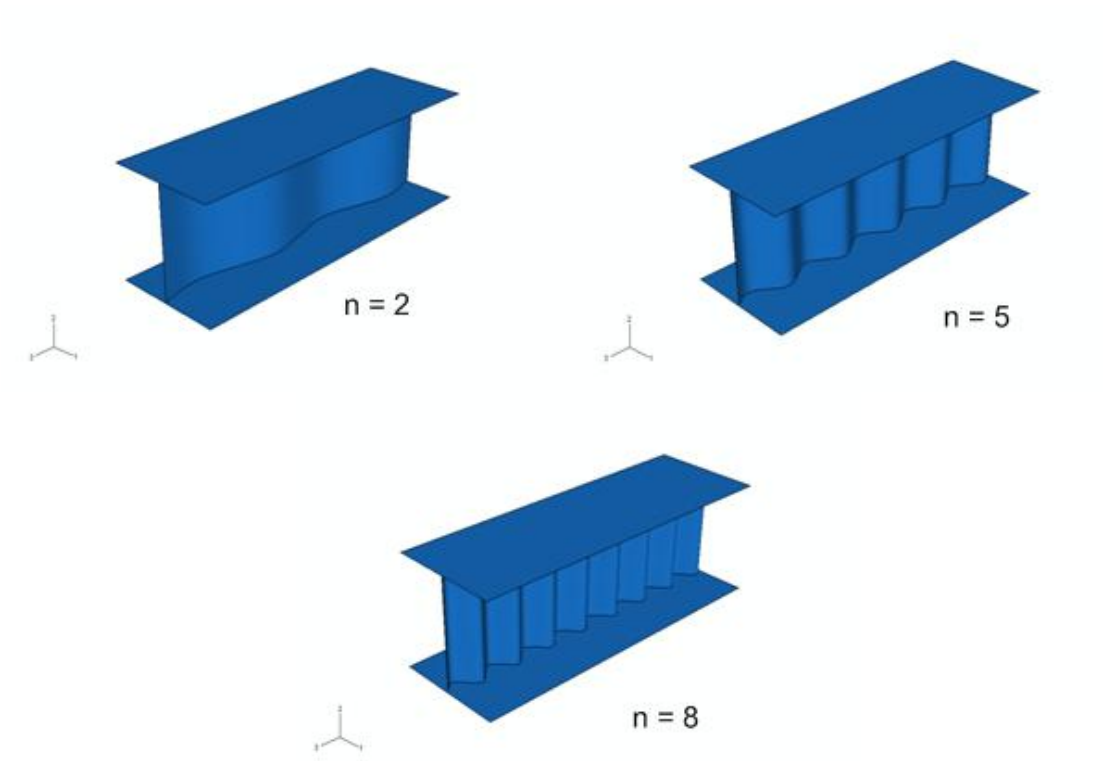

Figure 3.3.1: Sine Wave Beam Geometries with Two, Five, and Eight Periods and Web Amplitude of Twenty Millimeters.

The mean crushing force-deflection response for each beam configuration is given in Figure 3.3.2, where some interesting observations can be made.

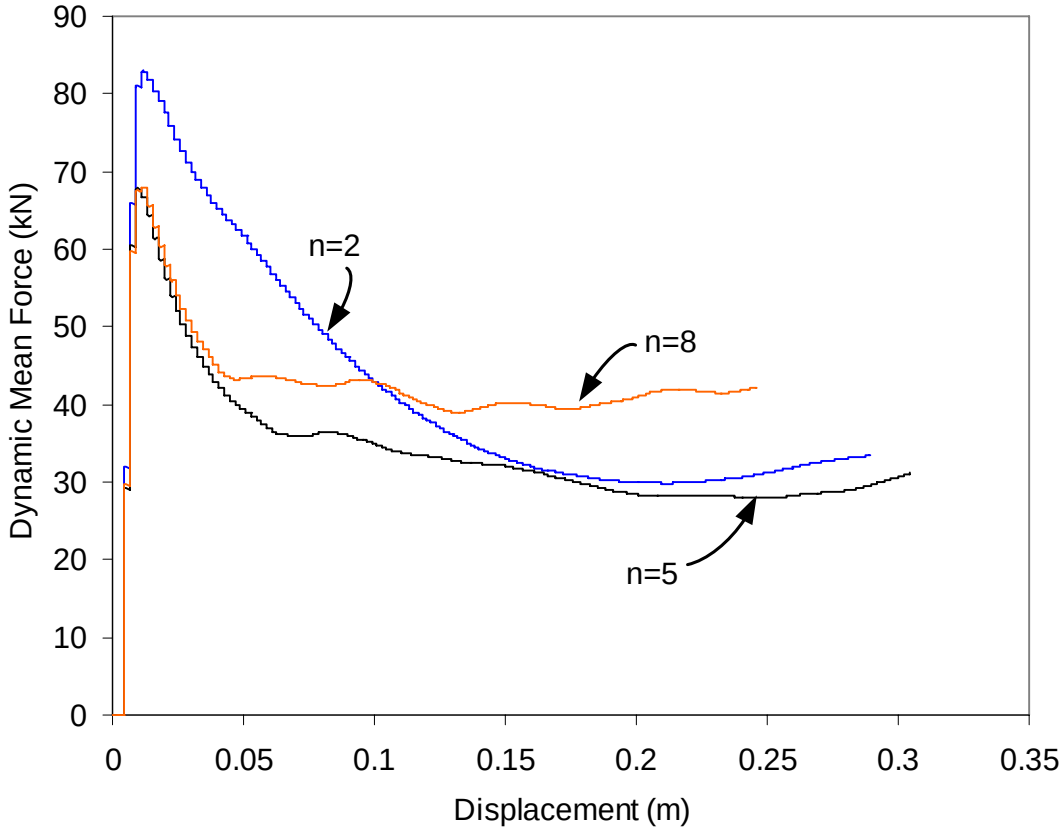

Figure 3.3.2: Dynamic Mean Force Versus Deflection for a SWB Having Web Amplitude of Twenty Millimeters and Period Numbers of Two, Five, and Eight.

The period number has a significant effect on the dynamic mean crushing force response of the SWB of twenty millimeter web amplitude. The force of the two-period beam is much greater during the initial crushing of the beam. However, the force response falls off very rapidly once the prescribed buckling mode becomes dominant. The kinetic energy absorption-deflection response is given in Figure 3.3.3.

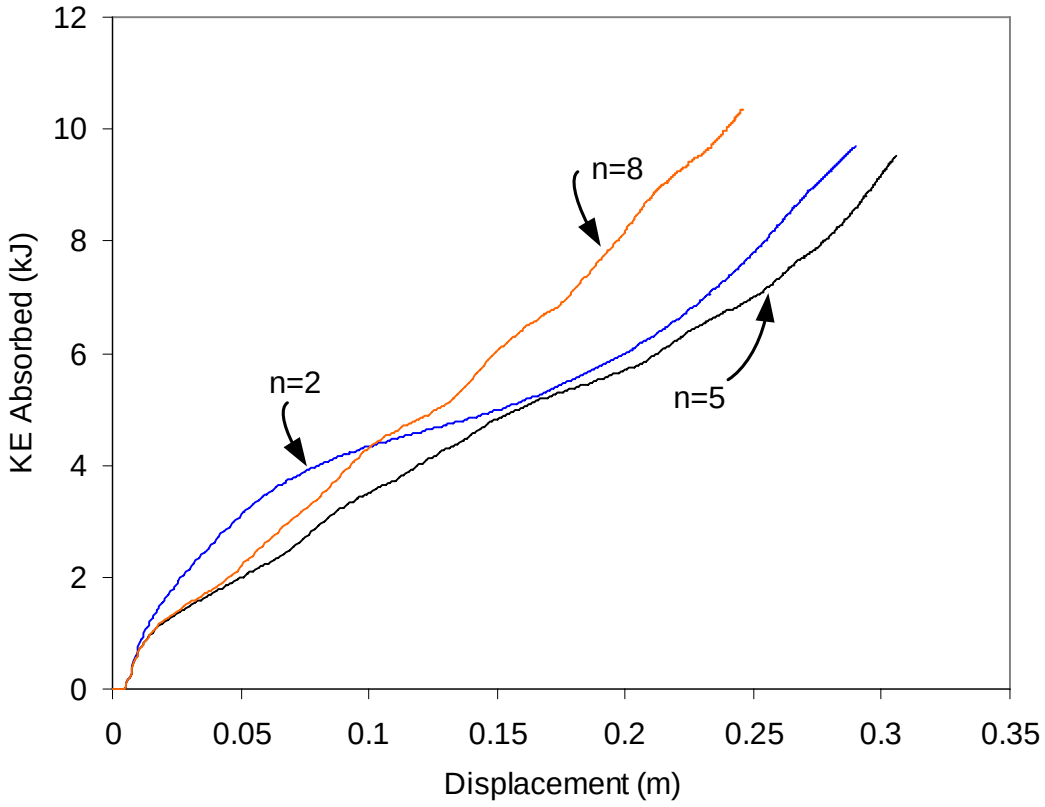

Figure 3.3.3: Absorbed Kinetic Energy Versus Deflection for a SWB Having Web Amplitude of Twenty Millimeters and Period Numbers of Two, Five, and Eight.

An interesting phenomenon occurs in the two previous plots. As shown in Figure 3.3.3, the rate of kinetic energy absorption for the two-period beam is initially higher than the other two structures. This declines rapidly at the crush distance of 0.06 meters. Upon initial impact with the rigid wall, the beam begins to deform locally by wrinkling. This localized deformation yields greater energy absorption from the severe plastic strain experienced. After the crush distance reaches 0.06 meters, the prescribed buckling mode emerges and dominates the remainder of the crush length. The crush progression of the 20 mm web amplitude beam having two periods is illustrated in Figure 3.3.4.

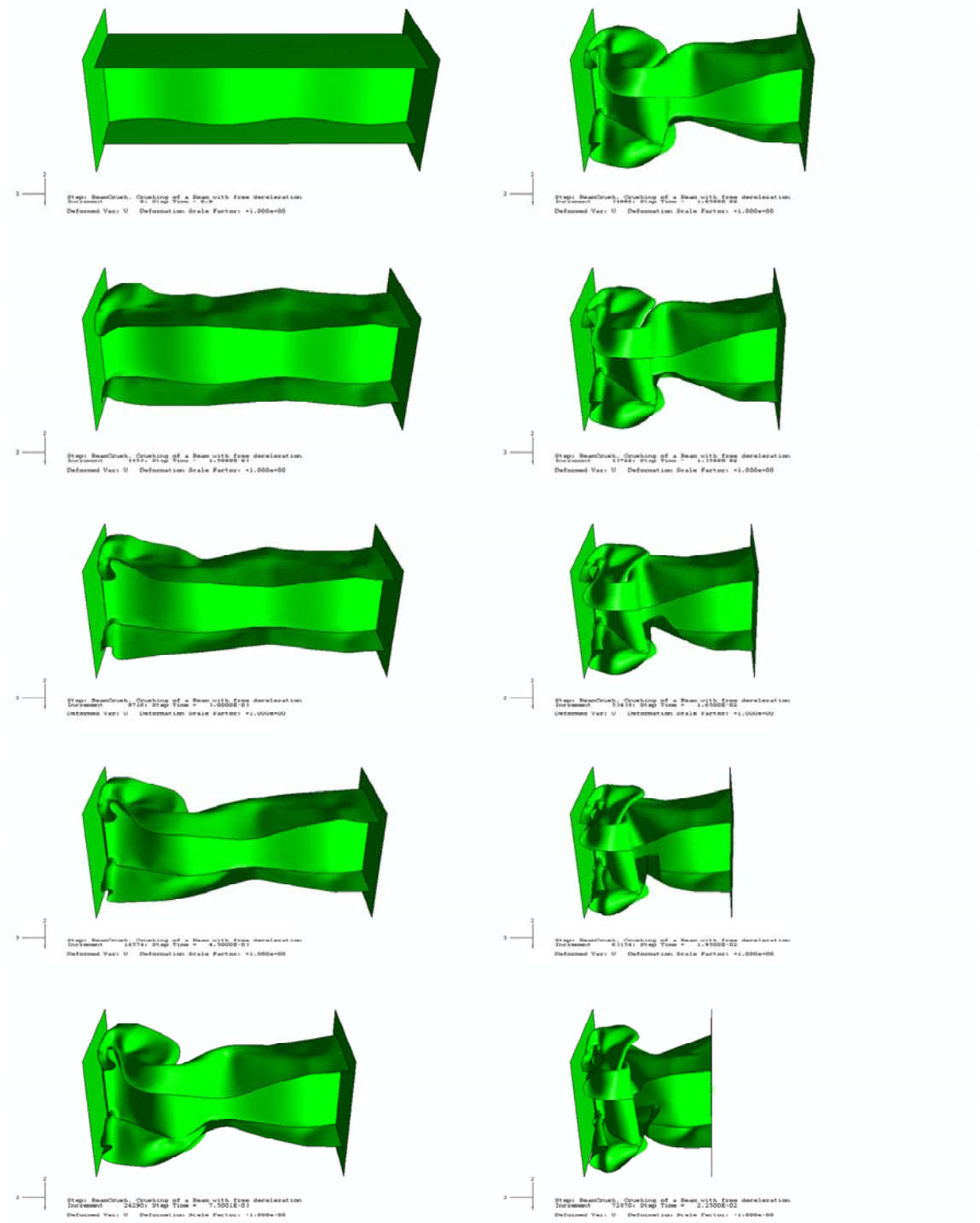

Figure 3.3.4: Axial Crush Progression of a SWB with Web Amplitude of Twenty Millimeters, Two Periods and Thickness of 1.5 Millimeters.

With this localized deformation, the final kinetic energy absorption for the two period beam was actually higher than that of the five period beam. For a web amplitude of 20 mm, the weight increase from two periods to five periods is only 4% but, from two periods to eight periods yields an increase of 10%.

3.3.2 Effect of period number with web amplitude of forty millimeters

Period number's effect was next studied using web amplitude of 40 millimeters, with two, five, and eight periods. The geometry of each beam is given in Figure 3.3.5.

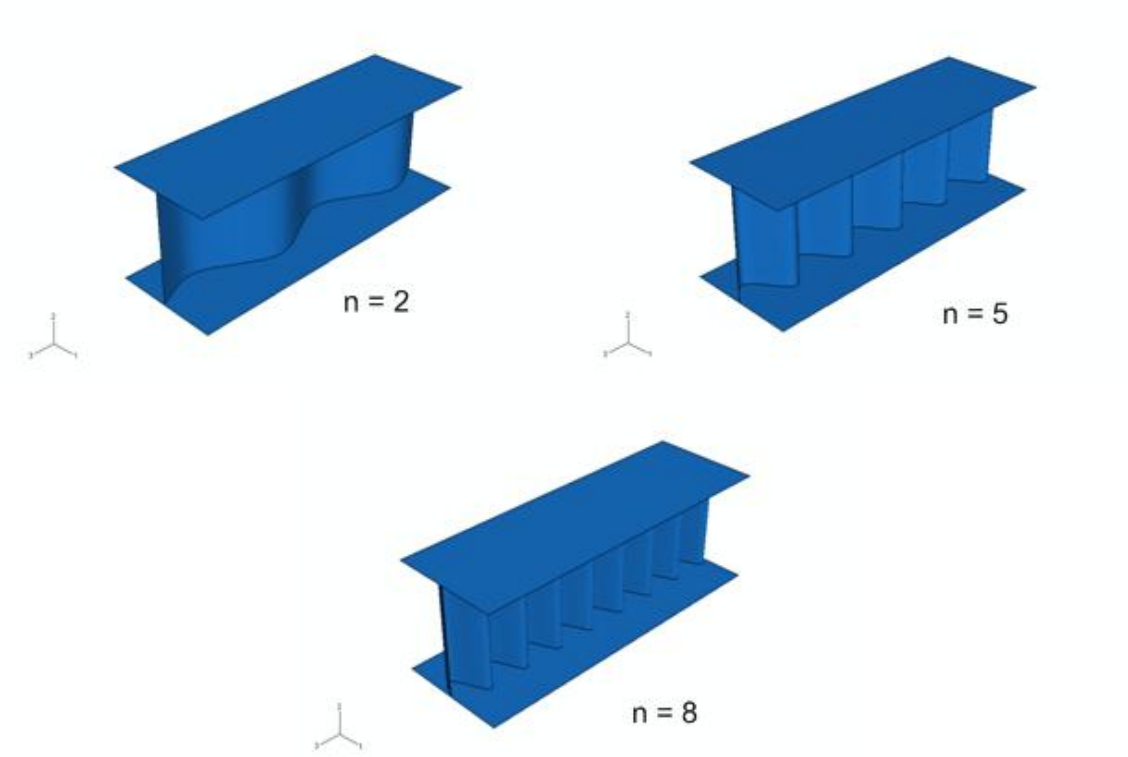

Figure 3.3.5: Sine Wave Beam Geometries with Two, Five, and Eight Periods, and Web Amplitude of Forty Millimeters.

The mean crushing force-displacement and kinetic energy absorption-displacement responses are given in Figures 3.3.6 and 3.3.7, respectively.

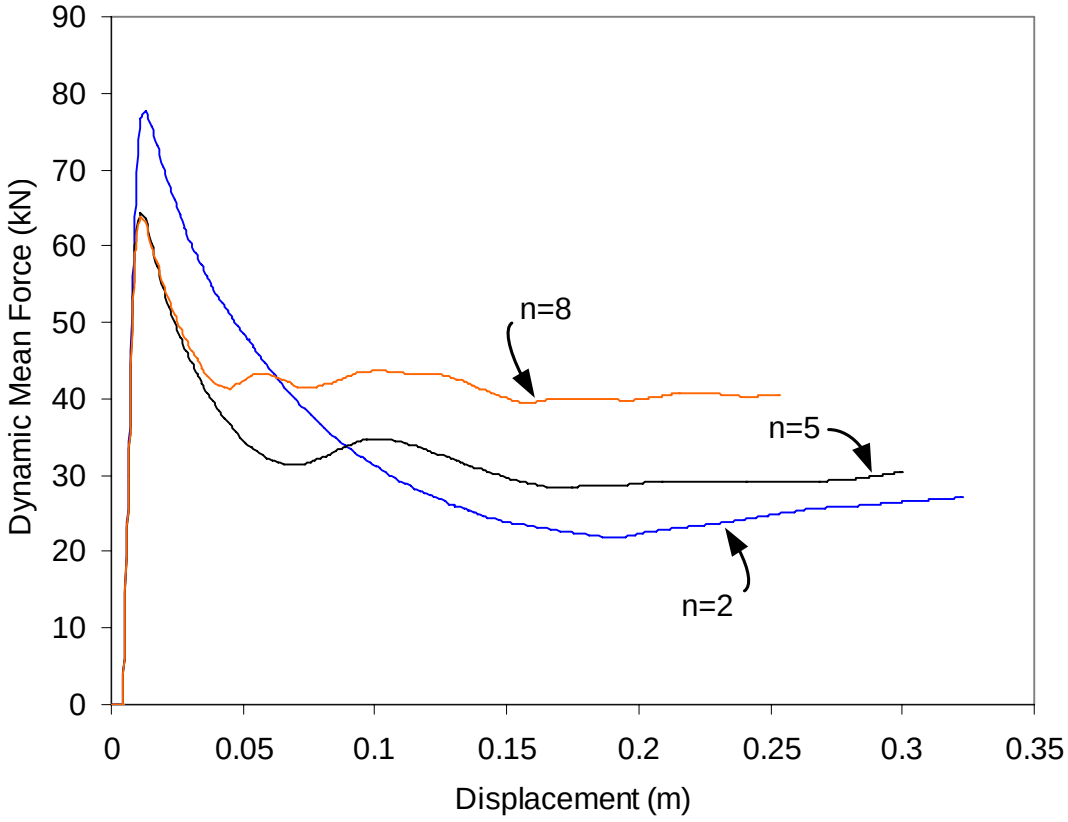

Figure 3.3.6: Dynamic Mean Force Versus Deflection for a SWB Having Web Amplitude of Forty Millimeters and Period Numbers of Two, Five, and Eight.

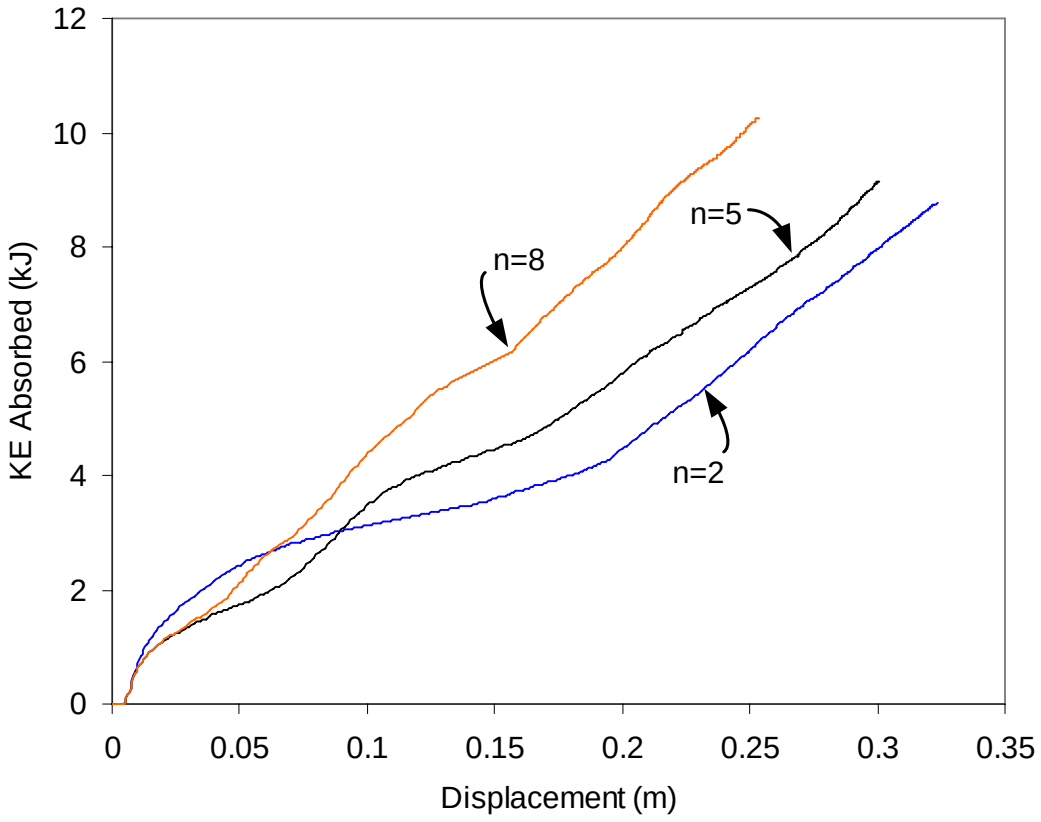

Figure 3.3.7: Absorbed Kinetic Energy Versus Deflection for a SWB Having Web Amplitude of Forty Millimeters and Period Numbers of Two, Five, and Eight.

As with the 20 millimeter web amplitude, the 40 millimeter web amplitude beam having two periods initially absorbs more energy per unit crush length. Once again, this declines rapidly upon the initialization of the prescribed buckling mode. The mode initiates earlier in this beam than the 20 millimeter beam since the increased web amplitude causes decreased local deformation. Once the prescribed buckling mode initiates, higher period number results in higher energy absorption of the structure.

3.3.3 Effect of period number with web amplitude of sixty millimeters

The third study of period number was performed using a web amplitude of sixty millimeters. Again 2, 5, and 8 periods were used and the corresponding geometry of each beam is depicted in Figure 3.3.8.

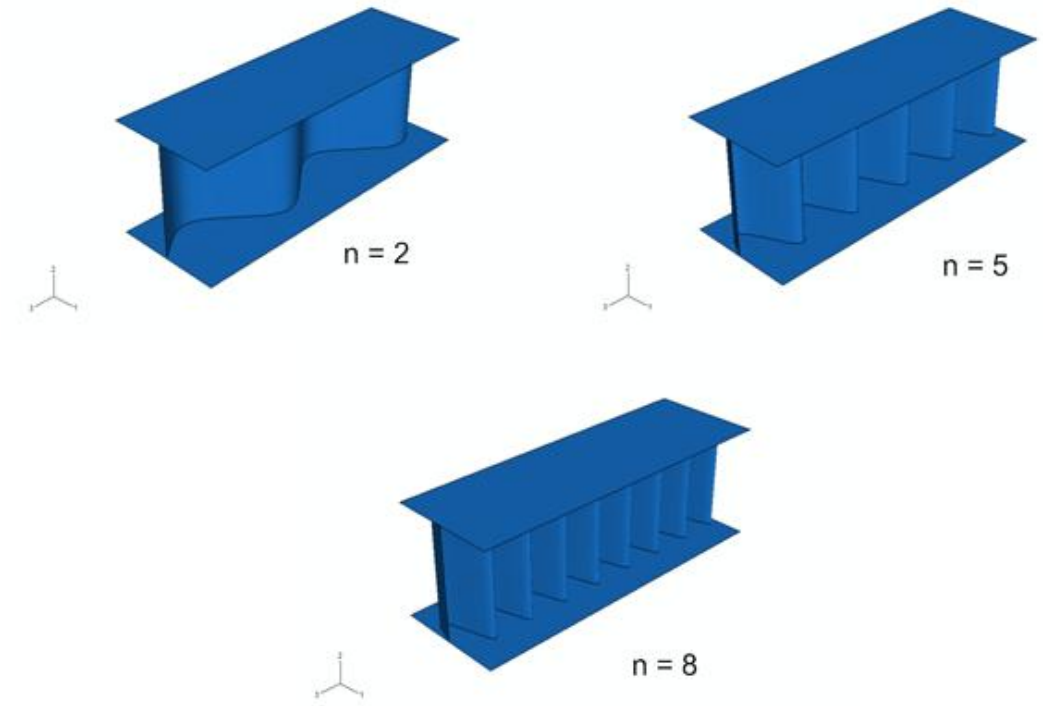

Figure 3.3.8: Sine Wave Beam Geometries with Two, Five, and Eight Periods, and Web Amplitude of Sixty Millimeters.

The responses of dynamic mean force and kinetic energy versus crush distance are given in Figures 3.3.9 and 3.3.10, respectively.

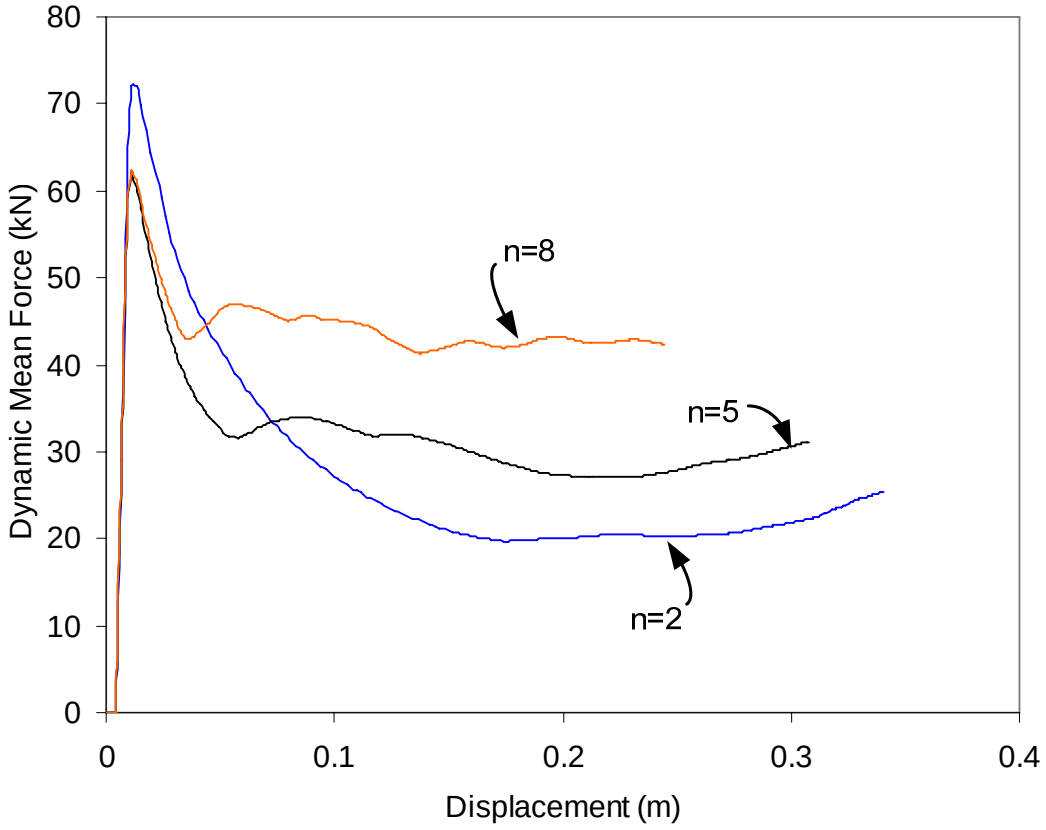

Figure 3.3.9: Dynamic Mean Force Versus Deflection for a SWB Having Web Amplitude of Sixty Millimeters and Period Numbers of Two, Five, and Eight.

The dynamic mean force is initially highest for the structure having two periods; however it quickly decreases below the other two structures. The energy absorption rate is higher initially for the two period-beam but again drops below the other two.

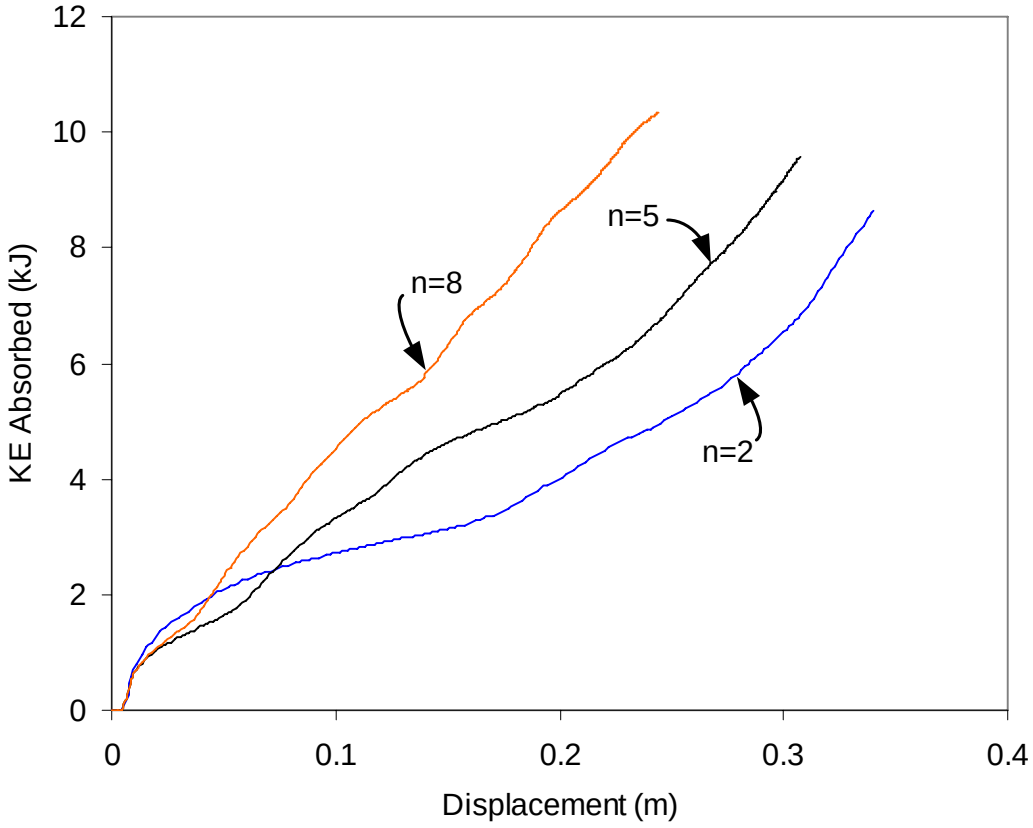

Figure 3.3.10: Absorbed Kinetic Energy Versus Deflection for a SWB Having Web Amplitude of Sixty Millimeters and Period Numbers of Two, Five, and Eight.

A general trend is present when looking at the performance of the 20, 40, and 60 millimeter web amplitude beams. The five and eight period beams consistently perform similar to each other, while the two period beam performance changes drastically depending on web amplitude. The greater the web amplitude, the less kinetic energy absorbed by the two period beam.

3.3.4 Effect of period number with web amplitude of eighty millimeters

The final parametric test was performed with web amplitude of eighty millimeters. The geometry of each model is featured in Figure 3.3.11.

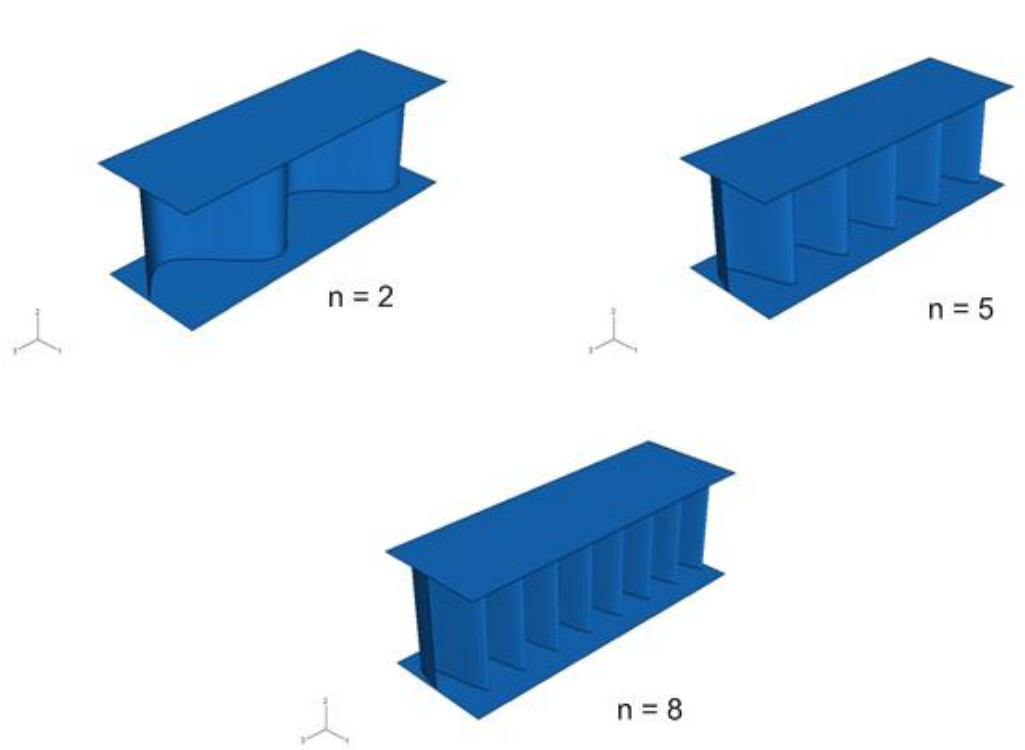

Figure 3.3.11: Sine Wave Beam Geometries with Two, Five, and Eight Periods, and Web Amplitude of Eighty Millimeters.

At web amplitude of eighty millimeters, there is a considerable increase in the amount of material present with increasing period number. The two period beam weighs 2.08 kg, the five period beam weighs 2.70 kg, and the eight period beam weighs 3.40 kg. Figure 3.3.12 gives the dynamic mean crushing force-displacement response for these beam configurations.

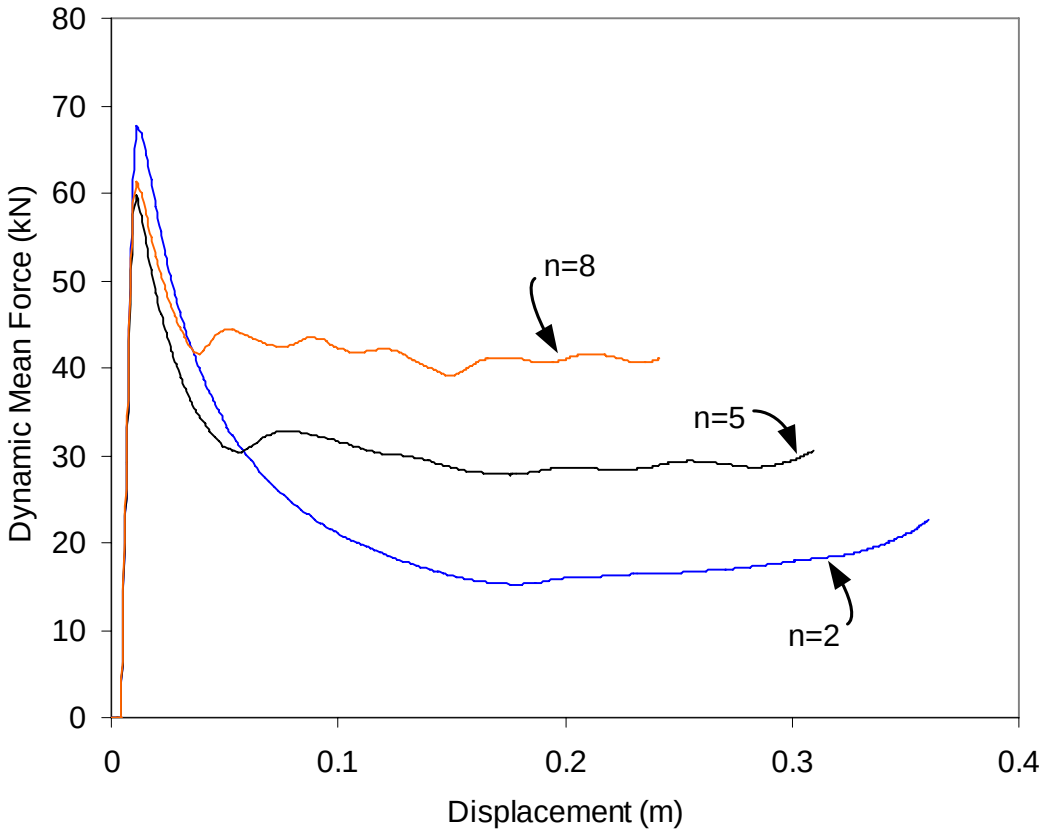

Figure 3.3.12: Dynamic Mean Force Versus Deflection for a SWB Having Web Amplitude of Eighty Millimeters and Period Numbers of Two, Five, and Eight.

The number of periods has a very significant effect on the dynamic mean force of the beam with eighty millimeter web amplitude. The mean force drops drastically once the prescribed buckling mode engages.

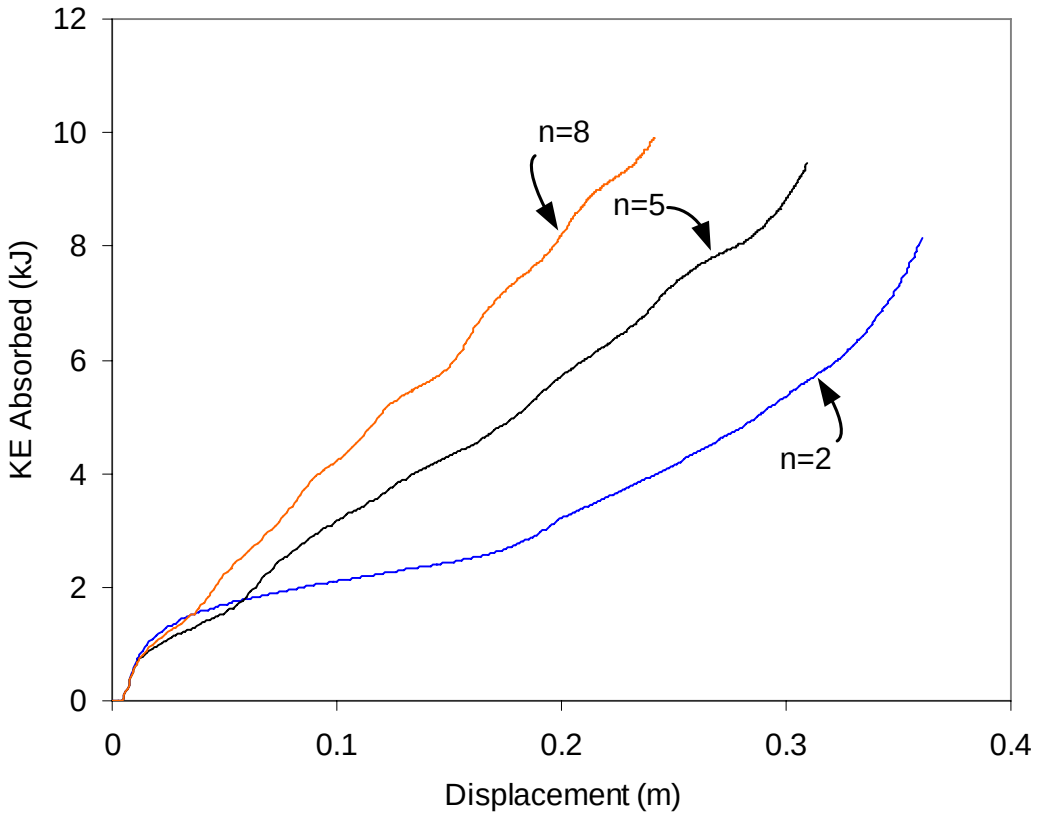

Figure 3.3.13: Absorbed Kinetic Energy Versus Deflection for a SWB Having Web Amplitude of Eighty Millimeters and Period Numbers of Two, Five, and Eight.

The two previously given plots indicate that period number has the largest effect on energy absorption when the web amplitude is eighty millimeters. Initial wrinkling of the upper and lower plates is virtually nonexistent for the two period beam. Instead the prescribed buckling mode initiates immediately upon impact. The eight period beam with eighty millimeter web amplitude beam performs the same as the previous three web

amplitudes. With five period beams as a whole, the energy absorption is less than the eight period beams, by almost the same amount in each configuration. As observed in Figures 3.3.3, 3.3.7, 3.3.10, and 3.3.13, the difference in energy absorption between the five and eight period beams is almost identical, with eight period structures absorbing more energy per unit crush length than five period-structures. With this increase in energy absorption, there is also an increase in weight. The energy absorbed per unit mass in the eighty millimeter web amplitude beam with two periods is 3.91 kJ/kg, five periods 3.50 kJ/kg, and eight periods is 2.91 kJ/kg. There is a significant difference in these numbers but the application of the energy absorber will truly dictate the necessary geometric features.

3.4 Comparison of SWB to Prismatic Structures

The final results presented here compare the performance of the SWB to the prismatic structures. The geometries of the prismatic structures are featured in Figure 3.4.1. For all configurations of the SWB, the energy absorption per unit length was lower than that of the prismatic structures. That being said, the force felt by the impacting body was also less in the SWB configurations for the entire duration of the impact.

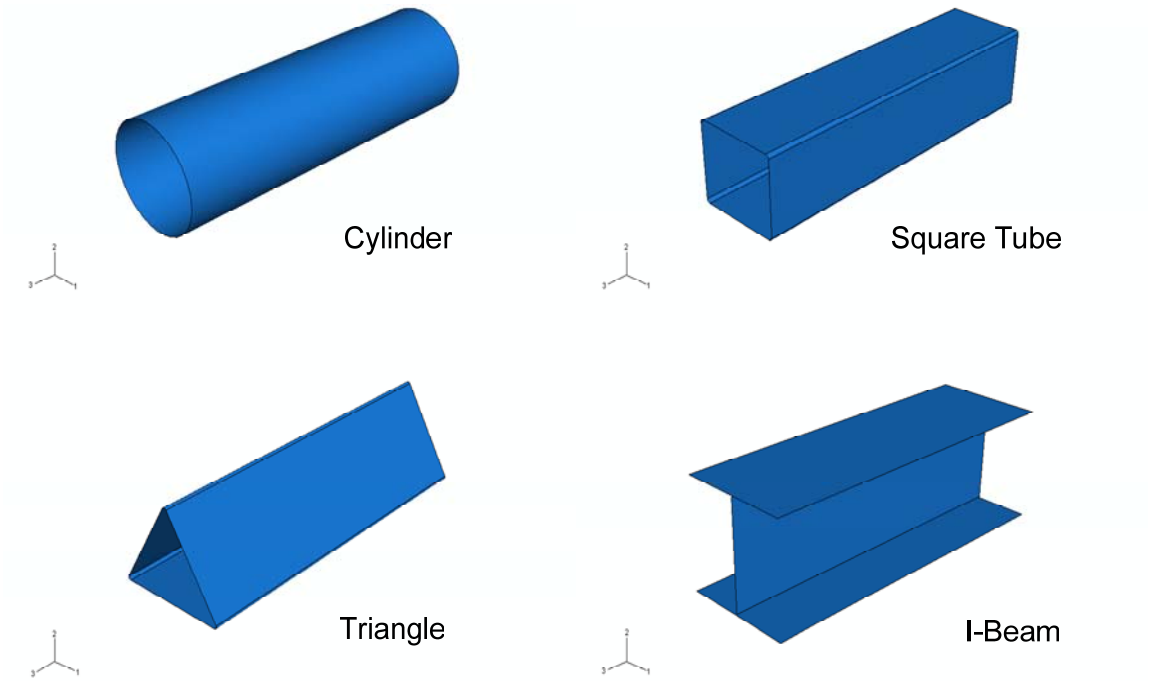

Figure 3.4.1: Geometric Configurations of Prismatic Structures with Equal Cross Sectional Areas.

To obtain comparable results between the various geometries, a uniform volume of material was used in each prismatic structure. Sun et al. (2004) used this approach to compare tubes of different cross sectional shapes. The task is accomplished by setting the perimeters of each cross section equal to one another, since the length and thickness are also held constant. The value for perimeter is 400 mm, the length is 400 mm, and the thickness is 1.5 mm. These values for length and thickness are equal for all structures presented in this final section. The impacting mass and velocity are also equal for each impact and the values are 90 kilograms, and fifteen meters per second, respectively. The dynamic mean crushing force-displacement and absorbed kinetic energy-displacement responses for every structure are presented in Figures 3.4.2 and 3.4.3, respectively.

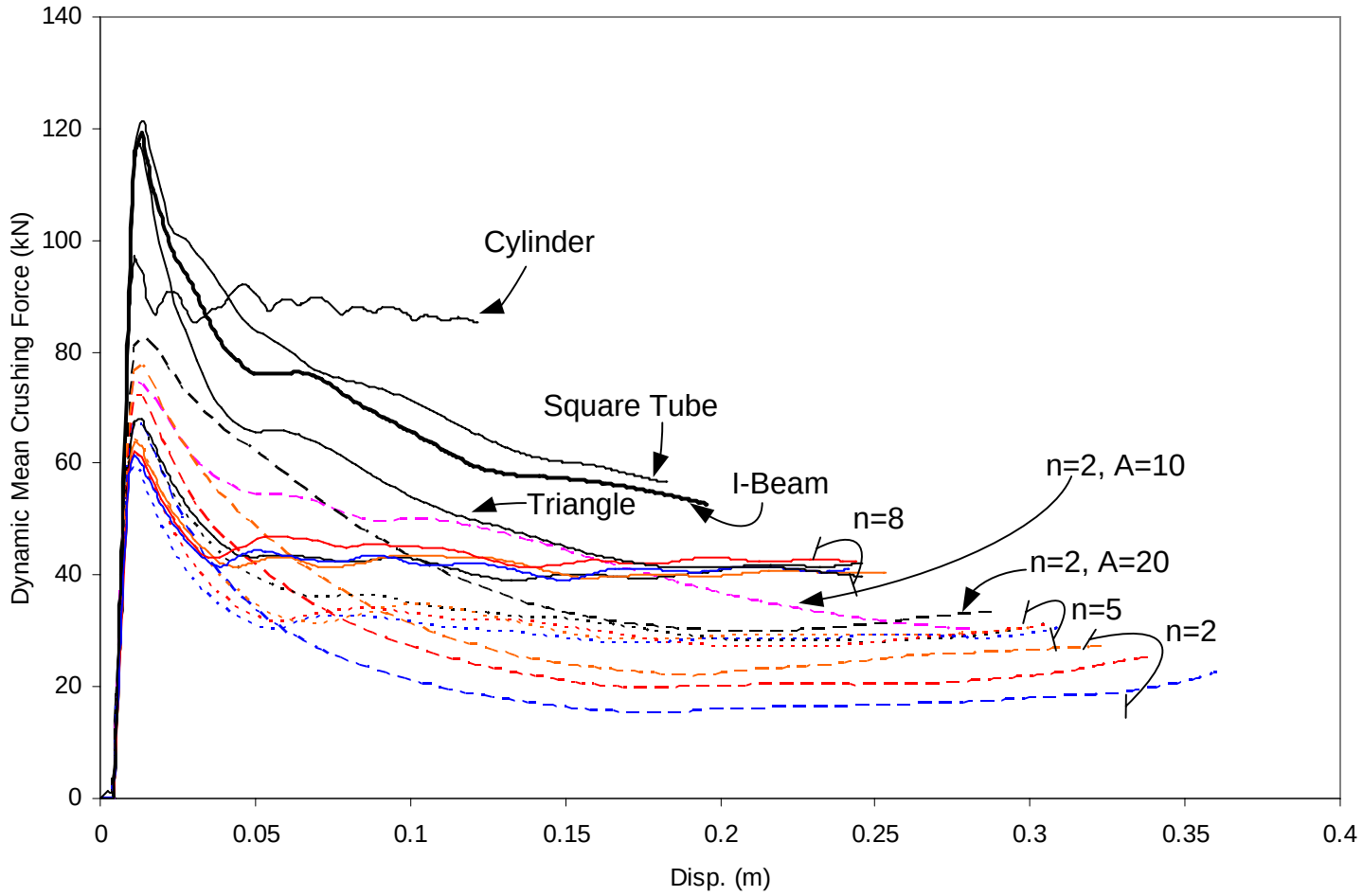

Figure 3.4.2: Dynamic Mean Crushing Force Versus Deflection for All Structures Tested.

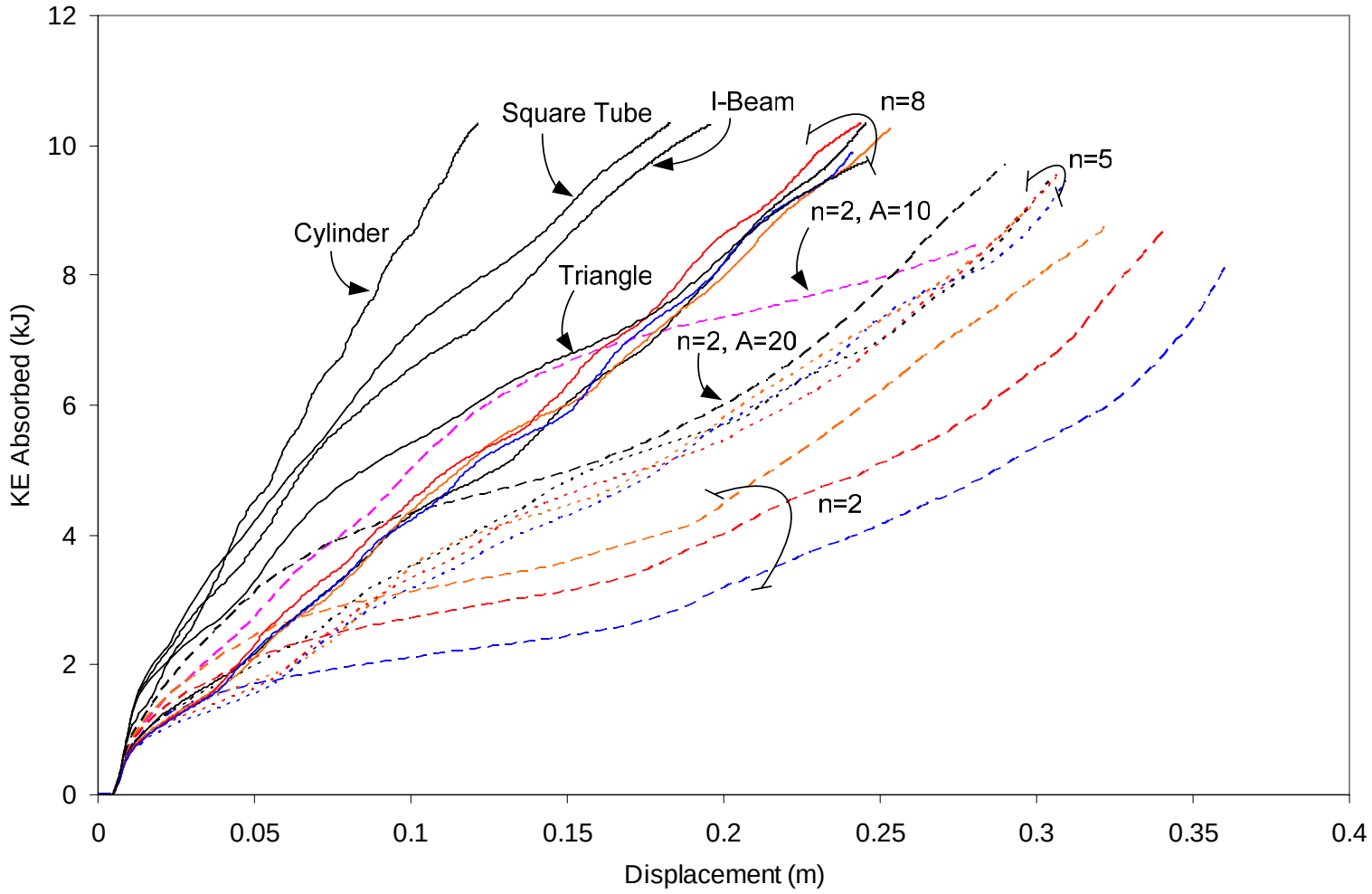

Figure 3.4.3: Absorbed Kinetic Energy Versus Displacement for All Structures Tested.

From the previous two plots, a banding formation can be seen in the SWB responses. The banding takes place with the structures having the same period numbers. With two exceptions, the eight period SWBs have the highest energy absorbed per unit length compared to the five and two period beams. The exceptions occur in the SWBs having two periods and web amplitudes of 10 and 20 mm. In these cases the energy absorbed per unit length is higher. Only after their prescribed buckling modes engage, do their performances fall below that of the eight period beams. This is a significant observation since it shows how much effect the prescribed buckling mode has on the structure.

The peak force for each of the prismatic structures tested is significantly higher than for any of the SWBs. Of the SWB models, the structure having two periods and web amplitude of 20 mm has the highest peak force with a value of 185 kN. Of the prismatic structures, the square tube has the lowest peak force with a value of 233 kN. Since a lower peak force results in less deceleration and a decreased likelihood of passenger injury, these best and worst case scenarios for the prismatic and SWB, respectively, are significant. In addition to the peak force, the mean crushing force for the prismatic structures, with the exception of the triangular cross section with crush lengths exceeding 0.17 m, are higher than for the SWBs. A lower mean crushing force will also result in a lower force felt by the passengers during the entirety of the crushing process. The peak force, mean crushing force, and stroke efficiency values are given in Table 3.4.1. Recall that stroke efficiency is defined as crush length divided by the original, undeformed length of the absorber, and higher values are desirable for improved crashworthiness.

Table 3.4.1: Various energy absorption properties for SWB and prismatic structures.

Model	Mean Crushing Force (kN)	Peak Force (kN)	Mass of Model (kg)	Stroke Efficiency
Cylinder	85.02	236.863	1.87	0.304
I-Beam	52.76	235.841	1.88	0.489
n=2, A=10	30.05	178.523	1.88	0.705
n=2, A=20	33.44	185.043	1.89	0.725
n=2, A=40	27.12	160.088	1.94	0.808
n=2, A=60	25.44	155.957	2.00	0.851
n=2, A=80	22.57	162.886	2.08	0.901
n=5, A=20	31.16	168.002	1.97	0.763
n=5, A=40	30.45	169.042	2.17	0.750
n=5, A=60	31.18	166.820	2.42	0.769
n=5, A=80	30.53	166.826	2.70	0.774
n=8, A=20	42.15	172.149	2.08	0.614
n=8, A=40	40.50	162.823	2.47	0.633
n=8, A=60	42.39	167.793	2.92	0.610
n=8, A=80	41.02	170.058	3.40	0.603
Square Tube	56.58	232.915	1.84	0.456
Triangle	41.50	253.529	1.81	0.614

A higher value for stroke efficiency is found in the SWB models as compared to the prismatic structures. This means the crushing process deforms a larger portion of the SWB than of a prismatic structure. Effectively, a lower stroke efficiency for a structure that absorbs a similar amount of energy means that less crush distance was needed. If the absorber is crushed over a longer distance, the resulting force will be smaller if the energy absorbed will be the same. According to the work-energy theorem it will take the same amount of work to deform the absorber if the net change in kinetic energy is equal. Spreading this work over a longer distance reduces the required force magnitude, reflected in the previous table with the mean crushing force. With a lower force felt on the impacting body, a lesser chance of passenger injury results.

4. CONCLUSIONS

A sine wave beam was investigated for use as an energy absorbing structure subject to axial crushing under impact loading. The energy absorbing properties of the beam were studied parametrically with variations in the thickness, web amplitude, and period number along the length of the structure. These analyses were performed using the ABAQUS suite to solve for the complex deformations that result from crushing under the impact loading. The results of the parametric studies were compared to each other, and then to the performance of typical prismatic structures. The reaction force versus displacement was used as a basis for comparison between the SWB and prismatic structures. Using the dynamic mean crushing force versus displacement and absorbed kinetic energy versus displacement responses, the performance was evaluated and conclusions were drawn. The results indicate that introducing the sinusoidally shaped web between the upper and lower plates of the beam allows the crushing mode to be controlled based on the web's shape. This confirms the hypothesis that was proposed initially.

Sine wave beams having five periods and web amplitude of forty millimeters were used to investigate the effect of variations in thickness of the web and flanges. Increased thickness produces higher energy absorption per unit crush length, with higher dynamic mean force. As the thickness of the upper and lower flanges increases, their deformation becomes more predictable and the folds smoother and shallower. The stroke also decreases with increasing thickness, leading to an increase in force experienced by the impacting body.

The effect of web amplitude was also studied keeping thickness and period number the same. It was found that as web amplitude increases, the dynamic mean force decreases. However, upon reaching a certain period number, approximately five, the effect of the amplitude diminishes and the performance of beams with equal period number becomes nominally the same. Therefore, the beam with small amplitude would be the preferable structure due to the decrease in weight over the larger amplitude beams. Also, as the wave amplitude approaches zero, the energy absorbing performance of the beam approaches that of a prismatic I-beam structure. This observation shows the idea of the sinusoidally shaped web allowing more control of the crush deformation.

The effect of period number was studied using constant web amplitude and thickness. In general the period number has a significant effect on the energy absorbing performance. With two periods, a combined deformation mode occurs with localized wrinkling occurring in addition to smoother deformation in the prescribed buckling mode. For web amplitude 20 mm or less, the two-period beams have higher energy absorption than the five period and eight period beams. For beams having web amplitude of 40 mm and larger, the result is an increase in energy absorption corresponding to an increase in period number.

Comparison of the performance of the SWB and the prismatic structures yielded some interesting observations. Generally speaking the energy absorption per unit length for all SWB configurations was lower than that of the prismatic structures. Conversely, the peak and dynamic mean reaction forces felt on the impacting body were also less. The stroke efficiency was high for each SWB tested, meaning that the crushing process utilized more of the available crushing length of the absorber. Through further

optimization, this force may be further reduced while retaining the beneficial energy absorbing qualities of the SWB.

5. FUTURE WORK

The energy absorbing ability of various geometrical shapes was investigated using a finite element analysis package. This research could be extended in the following directions:

1) An investigation into the other parameters in the sine wave beam, mentioned in Chapter 2, should be performed. This investigation should include a study into the interactions between each of the parameters, since it is highly unlikely that each one will act independently of the others under all conditions.

2) An investigation should be conducted into the use of different materials, specifically anisotropic materials, such as carbon fiber composites. These should be subjected to the same geometrical shapes, boundary, and loading conditions. Composite materials are comparable to isotropic materials in energy absorption capacity vs. weight due to their high in-plane, tensile strength and their relatively low density.

3) Experimental testing on the sine wave beam geometries should be performed in a laboratory environment.

4) Sine wave beams should be evaluated under oblique loading conditions. Energy absorbing structures need to be able to perform under non-axial crushing conditions.

5) The addition of a cellular material to the interior of the beam should be considered. A cellular structure could be placed on either side of the web, or between two parallel sine wave webs, to help oppose the large plastic deformation of the upper and lower plates.

6) An investigation should be performed on the imperfection sensitivity of the sine wave beam to the initial imperfections introduced into the computational model.

REFERENCES

1. Lu, G. and Yu, T.X., 2003, *Energy Absorption of Structures and Materials*, Woodhead Publishing Limited: Cambridge England, Boston, New York, Washington DC.

2. Johnson, W., and Yu, T.X., 1989, "An Outline of Engineering Dynamic Elasticity and Plasticity," *Plasticity and Modern Metal-Forming Technology* (ed. T.Z. Blazynski), Elsevier, New York, pp. 73-114.

3. Nagel, G., 2005, "Impact and Energy Absorption of Straight and Tapered Rectangular Tubes," PhD Dissertation, Queensland University of Technology, Brisbane, Australia.

4. Abramowicz, W., and Jones, N., 1984, "Dynamic Axial Crushing of Circular Tubes," *International Journal of Impact Engineering*, pp. 263-281.

5. Abramowicz, W., and Jones, N., 1986, "Dynamic Progressive Buckling of Circular and Square Tubes," *International Journal of Impact Engineering*, pp. 243-270.

6. Reid, S.R., and Reddy, T.Y., 1986, "Static and Dynamic Crushing of Tapered Sheet Metal Tubes of Rectangular Cross-Section," *International Journal of Mechanical Sciences*, Vol. 28, pp. 623-637.

7. Reid, S.R., Reddy, T.Y., and Gray, M.D., 1986, "Static and Dynamic Axial Crushing of Foam-Filled Sheet Metal Tubes," *International Journal of Mechanical Sciences*, Vol. 28, pp. 295-322.

8. Jones, N., 2001, "Dynamic Material Properties and Inelastic Failure in Structural Crashworthiness," *International Journal of Crashworthiness*, Vol. 6, pp. 7-18.

9. Jones, N., 1999, "Some Phenomena in the Structural Crashworthiness Field," *International Journal of Crashworthiness*, Vol. 4, pp. 335-350.

10. Jones, N., 1989, *Structural Impact*, Cambridge University Press: Cambridge, UK.

11. Farley, G.L., 1992, "Relationship between Mechanical-Property and Energy-Absorption Trends for Composite Tubes," *Vehicle Structures Directorate*, Hampton, VA.

12. Abramowicz, W., 2003, "Thin-Walled Structures as Impact Energy Absorbers" *Thin-Walled Structures*, Vol. 41, pp. 91-107.

13. Alghamdi, A., 2001, "Collapsible Impact Energy Absorbers: An Overview," *Thin-Walled Structures*, Vol. 39, pp. 189-213.

14. Sun, J., Ekwaro-Osire, S., Hsiang, S.M., "Comparison and Optimization of Impact Behavior of Triangular Tubes," AIAA Paper no. 2004-4575, August-September 2004.

15. Pinho, S.T., Camanho, P.P., de Moura, M.F., 2004, "Numerical Simulation of the Crushing Process of Composite Materials," *International Journal of Crashworthiness*, pp. 263-276.

16. Song, Hong-Wei, Wan, Zhi-Min, Xie, Zhi-Min, and Du, Xing-Wen, 2000, "Axial Impact Behavior and Energy Absorption Efficiency of Composite Wrapped Metal Tubes," *International Journal of Impact Engineering*, pp. 385-401.

17. Schultz, M.R., 1998, "Energy Absorption Capacity of Graphite-Epoxy Composite Tubes," MS Thesis, Virginia Polytechnic Institute and State University, Blacksburg, VA.

18. Farley, G.L., 1989, "Energy-Absorption Capability of Composite Tubes and Beams," PhD Dissertation, Virginia Polytechnic Institute and State University, Blacksburg, VA.

19. Mamalis, A.G., Manolakos, D.E., Baldoukas, A.K., and Viegelahn, G.L., 1989, "Deformation Characteristics of Crashworthy Thin-Walled Steel Tubes Subjected to Bending," *Proceedings Institution of Mechanical Engineers Part C*, Vol. 203, pp. 411-417.

20. Mamalis, A.G., Manolakos, D.E., Ioannidis, M.B., Kostazos, P.K., and Hassiotis, G., 2001, "Finite Element Simulation of the Axial Collapse of Thin-Wall Square Frusta," *International Journal of Crashworthiness*, Vol. 6, pp. 155-164.

21. Gibson, L.J., and Ashby, M.F., 1997, *Cellular Solids, Structure and Properties*, 2nd ed., Cambridge University Press: Cambridge, UK.

22. Abramowicz, W., and Wierzbicki, T., 1988, "Axial Crushing of Foam-Filled Columns," *International Journal of Mechanical Science*, pp 263-271.

23. Børvik, T., Hopperstad, O.S., Reyes, A., Langseth, M., Solomos, G., and Dyngeland, T., 2003, "Empty and Foam-Filled Circular Aluminium Tubes Subjected to Axial and Oblique Quasi-Static Loading," *International Journal of Crashworthiness*, pp. 481-494.

24. Reddy, T.Y., and Wall, R.J., 1988, "Axial Compression of Foam-Filled Thin-Walled Circular Tubes," *International Journal of Impact Engineering*, pp. 151-166.

25. Heyerman, J.B., 2000, "On the Crashworthiness of Foam-Filled Ultralight Automotive Structures," MS Thesis, University of Toronto, Toronto, Ontario, Canada.

26. Reyes, A., Hopperstad, O.S., and Langseth, M., 2004, "Aluminum Foam-Filled Extrusions Subjected to Oblique Loading: Experimental and Numerical Study," *International Journal of Impact Engineering*, pp. 1645-1675.

27. Hibbitt, Karlsson, and Sorensen, Inc., 2006, *Getting Started with ABAQUS/Standard Version 6.6*, Pawtucket, RI.

28. Hibbitt, Karlsson, and Sorensen, Inc., 2006, *Getting Started with ABAQUS/Explicit Version 6.6*, Pawtucket, RI.

29. Hibbitt, Karlsson, and Sorensen, Inc., 2006, *ABAQUS/Analysis User's Manual, Version 6.6*, Pawtucket, RI.

30. Cook, Robert D., Malkus, David S., and Plesha, Michael E., 1989, *Concepts and Applications of Finite Element Analysis*, John Wiley & Sons: New York, Chichester, Brisbane, Toronto, Singapore.